

## Microphysical characterization of mixed-phase clouds

By ALEXEI V. KOROLEV<sup>1\*</sup>, GEORGE A. ISAAC<sup>1</sup>, STEWART G. COBER<sup>1</sup>, J. WALTER STRAPP<sup>1</sup> and JOHN HALLETT<sup>2</sup>

<sup>1</sup>Meteorological Service of Canada, Canada

<sup>2</sup>Desert Research Institute, USA

(Received 13 December 2001; revised 12 July 2002)

### SUMMARY

A detailed study of mixed-phase clouds associated with frontal systems obtained from a large dataset collected by the Convair 580 aircraft of the National Research Council (NRC) of Canada is presented. The total length of analysed in-cloud legs having total-water content (TWC)  $> 0.01 \text{ g m}^{-3}$  was about  $44 \times 10^3 \text{ km}$ . The ice–water fraction ( $\mu_3 = \text{ice-water content/TWC}$ ) had a minimum in the range  $0.1 < \mu_3 < 0.9$ , and two maxima for liquid clouds ( $\mu_3 < 0.1$ ) and ice clouds ( $\mu_3 > 0.9$ ). The concentration of particles in glaciated clouds was found to be nearly constant at  $2\text{--}5 \text{ cm}^{-3}$  for temperatures  $-35^\circ\text{C} < T < 0^\circ\text{C}$ . The concentration of droplets in liquid clouds decreased with decreasing temperature. The mean volume diameter of particles in ice clouds varied between  $20 \mu\text{m}$  and  $35 \mu\text{m}$ , and in liquid clouds between  $10 \mu\text{m}$  and  $12 \mu\text{m}$ . Both ice- and liquid-water content decreased with decreasing temperature. The results of this study may be used for validation of remote-sensing retrievals, and for weather- and climate-models.

KEYWORDS: Ice-particle concentration Ice-particle size Ice-water content

### 1. INTRODUCTION

Cloud droplets may stay in a metastable liquid condition down to about  $-40^\circ\text{C}$ . Below  $0^\circ\text{C}$ , populations of cloud particles may consist of a mixture of ice particles and liquid droplets. Such clouds are usually called ‘mixed-phase’ or ‘mixed’ clouds. Because of the difference of water vapour saturation over ice and over liquid, the mix of ice particles and liquid droplets is condensationally unstable and may exist only for a limited time. The relative proportion of water substance in the ice and liquid phases (the ‘phase composition’) of clouds is an important cloud microphysical parameter. The phase composition affects the rate of precipitation formation and the life cycle of clouds in general (e.g. Tremblay *et al.* 1996; Jiang *et al.* 2000). Knowledge of the mixed-phase in clouds is important for radar (e.g. Lohmeier *et al.* 1997), lidar (e.g. Young *et al.* 2000), satellite retrievals (e.g. Schols *et al.* 1999), radiation transfer calculations (e.g. Oshchepkov and Isaka 1998), and GCM and climate modelling (e.g. Sun and Shine 1995; Wilson 2000). The mixed phase is hypothesized to be one of the major causes for cloud electrification (e.g. Williams *et al.* 1991); it is also considered important for aircraft icing.

Studies of cloud phase-composition have been significantly limited by a lack of aircraft instruments capable of discriminating between the ice and liquid phases for a wide range of particle sizes. Early observations of mixed phase in clouds were collected with the help of airborne impactors and replicators (e.g. Zak 1937; Peppler 1940; Weickmann 1945; Borovikov *et al.* 1963). The processing of replicator and impactor measurements was plagued by fragmentation of ice particles and uncertainties related to collision efficiency. Nevertheless, these studies resulted in an important conclusion that liquid and ice particles may coexist in natural cold clouds down to  $-40^\circ\text{C}$ .

Moss and Johnson (1994) studied phase composition and derived ice-to-water ratios from images of cloud particles larger than  $125 \mu\text{m}$  as measured by a probe known as the Particle Measuring Systems (PMS) OAP-2DC. However, the errors in calculation of

\* Corresponding author: 28 Don Head Village Blvd, Richmond Hill, Ontario, L4C 7M6, Canada.  
e-mail: Alexei.Korolev@rogers.com

the water content which is in the ice phase, the ‘ice-water content’ (IWC), from two-dimensional particle images may reach a factor of two or three because of uncertainties in techniques of converting size to mass or area to mass (Korolev and Strapp 2002). The phase of a cloud particle is decided on the assumption that circular images are liquid droplets. Frozen droplets, depending on the supersaturation, may keep their spherical shape during some period following freezing. Moreover, a large variety of ice-particle images appear circular (Korolev *et al.* 2000; Cober *et al.* 2001b) and therefore may be misinterpreted as liquid.

Measurements of cloud liquid-water content (LWC) have become available following the development of the Johnson–Williams, King and Nevzorov LWC hot-wire probes (King *et al.* 1978; Nevzorov 1983). The development of aircraft instrumentation over the last two decades has significantly improved measurements of total (ice + liquid) water content (Nevzorov 1980; Brown 1993; Twohy *et al.* 1997). This has been an important step towards the study of mixed-phase clouds. Assessments of mixed-phase composition using hot-wire instruments have been conducted by Mazin *et al.* (1992), Korolev and Isaac (1998, 2000) and Cober *et al.* (2000, 2001b).

This work presents a study of the microphysical parameters in mixed-phase clouds based on aircraft in situ measurements. Statistics of cloud-particle sizes, concentration, total and liquid water content versus the mixed-phase composition for temperatures from 0 °C to –35 °C are presented.

## 2. INSTRUMENTATION

The Nevzorov probe is a constant-temperature hot-wire instrument consisting of two sensors: (1) for measurement of LWC and (2) for total (ice + liquid) water content (TWC). The Nevzorov LWC sensor has a cylindrical shape with the diameter of about 2 mm. The Nevzorov TWC sensor is a concave cone, having a diameter of 8 mm, which works as a trap for the impacting cloud particles. The threshold sensitivity to water and ice was estimated as 0.003 g m<sup>-3</sup> to 0.005 g m<sup>-3</sup>, discussed in detail in Korolev *et al.* (1998). The phase discriminating capability of the TWC and LWC sensors result from the difference in the behaviour of liquid and solid particles impacting on their surfaces. Small liquid droplets are flattened into a thin surface film after collision with the LWC or TWC collector sensors and completely evaporate. At the same time, ice particles tend to remain inside the conical hollow of the TWC collector until they melt and evaporate. In contrast, ice particles are assumed to break away from the convex cylindrical surface of the LWC collector with negligible heat expended relative to that for complete ice evaporation.

The phase discriminating capability of the Nevzorov probe was tested in the National Research Council (NRC) wind tunnel (Korolev *et al.* 1998). Figure 1 shows simultaneous measurements of the Nevzorov and Rosemount Ice Detector (RICE; BF Goodrich Aerospace Sensors Division\*) probes in a natural supercooled cloud (–5 °C ≤ *T* ≤ –12 °C). The periods when the RICE signal is oscillating or gradually increasing are indicative of the presence of supercooled liquid water. These periods are well correlated with the elevated Nevzorov LWC measurements in Fig. 1(b). For most of the time in-cloud TWC is larger than LWC (e.g. 20:15 UTC to 20:23 UTC), implying the presence of ice. When TWC is approximately equal to LWC, the cloud is considered primarily liquid (e.g. 20:23:50 UTC to 20:24:10 UTC).

\* Former Rosemount Company.

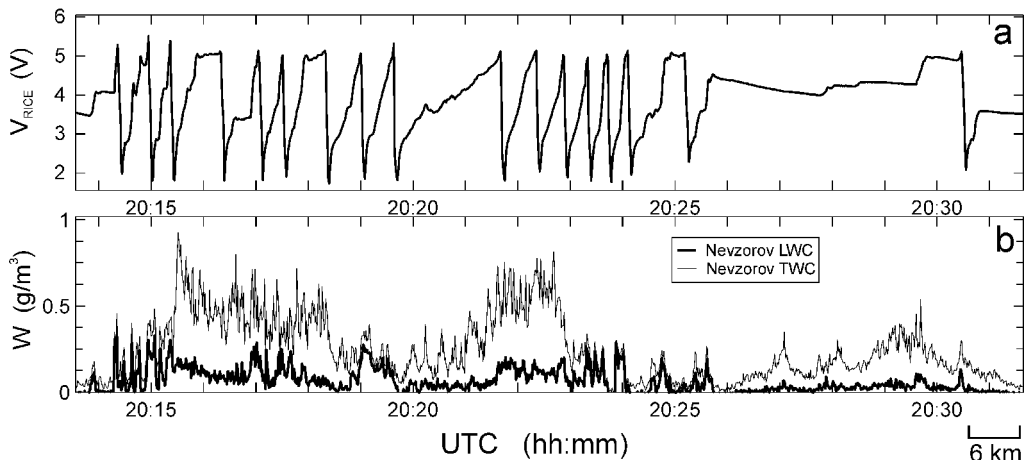


Figure 1. Simultaneous measurements: (a) Rosemount ice detector (RICE) probe and (b) Nevzorov liquid-water content (LWC) and total-water content (TWC) probes. The ratio between Nevzorov LWC and TWC characterizes different phase-composition of the cloud, e.g., mixed (20:15:00 UTC to 20:23:00 UTC), liquid (20:23:40 UTC to 10:24:10 UTC) and ice (20:25:45 UTC to 20:27:50 UTC). Third Canadian Freezing Drizzle Experiment (CFDE3), Ottawa, 11 February 1998, Altostratus/Nimbostratus,  $T = -5^{\circ}\text{C}$  to  $-12^{\circ}\text{C}$ ;  $H = 2300\text{ m}$  to  $4000\text{ m}$ .

The other cloud microphysical instrumentation relevant to this study includes: two Rosemount temperature-probes (BF Goodrich Aerospace Sensors Division) and a reverse flow temperature probe; a Cambridge dew-point hygrometer by EG&G International Inc. (EG&G); two Particle Measuring Systems Inc. (PMS) Forward Scattering Spectrometer Probes FSSP-100 (Knollenberg 1981), which measured droplet-size distributions in the  $2\text{--}32\ \mu\text{m}$  and  $5\text{--}95\ \mu\text{m}$  size ranges respectively; two PMS King probes (King *et al.* 1978); a PMS Optical Array Probe (OAP) OAP-2DC ( $25\text{--}800\ \mu\text{m}$ ); a PMS OAP-2DC Gray ( $25\text{--}1600\ \mu\text{m}$ ); and a PMS OAP-2DP ( $200\text{--}6400\ \mu\text{m}$ ) (Knollenberg 1981). The three PMS OAP probes provided shadow images and concentrations of hydrometeors within their respective size ranges.

These instruments were installed on the National Research Council (NRC) Convair 580 aircraft.

Regular maintenance and calibration of the FSSP probes were carried out in order to minimize the potential errors in droplet sizing. Dead-time losses and coincidence errors were taken into account during data processing. The data from each instrument were carefully examined for indications of fogging and ice build-up; such cases were excluded from the following analyses.

### 3. DATA PROCESSING

#### (a) Calculation of liquid- and ice-water content

Liquid-water content ( $W_{\text{liq}}$ ) and ice-water content ( $W_{\text{ice}}$ ) were calculated from the two following equations

$$W_{\text{TWC}} = \varepsilon_{\text{liqT}} W_{\text{liq}} + k\varepsilon_{\text{iceT}} W_{\text{ice}} \quad (1)$$

$$W_{\text{LWC}} = \varepsilon_{\text{liqL}} W_{\text{liq}} + \beta W_{\text{ice}}, \quad (2)$$

where  $W_{\text{TWC}}$  and  $W_{\text{LWC}}$  are the total- and liquid-water contents measured by the Nevzorov LWC and TWC sensors, respectively;  $\varepsilon_{\text{liqT}}$  and  $\varepsilon_{\text{iceT}}$  are the integrated collection efficiencies of liquid droplets and ice particles for the TWC sensor;  $\varepsilon_{\text{liqL}}$

is the integrated collection efficiency for liquid droplets for the LWC sensor;  $\beta$  is the coefficient accounting for the residual effect of the ice on the LWC sensor;  $k = L_{\text{ice}}^*/L_{\text{liq}}^*$  is the correction coefficient for the difference between expended specific energy of water evaporation ( $L_{\text{liq}}^*$ ) and ice sublimation ( $L_{\text{ice}}^*$ ).

The values of  $W_{\text{TWC}}$  and  $W_{\text{LWC}}$  were calculated as follows:

$$W_{\text{TWC}} = \frac{V_{\text{TWC}}^2}{UL_{\text{liq}}^* S_{\text{TWC}} R_{\text{TWC}}} \quad (3)$$

$$W_{\text{LWC}} = \frac{V_{\text{LWC}}^2}{UL_{\text{liq}}^* S_{\text{LWC}} R_{\text{LWC}}}. \quad (4)$$

Here  $V_{\text{TWC}}$  and  $V_{\text{LWC}}$  are the voltages measured across the TWC and LWC sensors having the resistances  $R_{\text{TWC}}$  and  $R_{\text{LWC}}$ , respectively;  $S_{\text{TWC}}$  and  $S_{\text{LWC}}$  are sample areas of the TWC and LWC sensors, respectively, and  $U$  is the true air speed.

For liquid clouds, the specific energy expended in heating and evaporating can be written as

$$L_{\text{liq}}^* = C_{\text{liq}}(T_e - T_a) + L_{\text{liq}}(T_e), \quad (5)$$

where  $C_{\text{liq}}$  is the specific heat of liquid water,  $T_a$  is the air temperature and  $L_{\text{liq}}(T_e)$  is the latent heat of evaporation of water at the evaporation temperature  $T_e$  (Nevzorov 1983; Korolev *et al.* 1998).

For ice particles

$$L_{\text{ice}}^* = C_{\text{ice}}(T_0 - T_a) + L_{\text{ice}} + C_{\text{liq}}(T_e - T_0) + L_{\text{liq}}(T_e), \quad (6)$$

where  $C_{\text{ice}}$  is the specific heat of ice,  $L_{\text{ice}}$  is the latent heat of fusion, and  $T_0 = 0^\circ\text{C}$ .

The evaporation temperature varies in the range  $T_c > T_e > T_a$ , where  $T_c$  is the temperature of the collector sensor ( $60^\circ\text{C} < T_c < 140^\circ\text{C}$ ). For simplicity it is convenient to use an average value of  $L_{\text{liq}}^* = 2.58 \times 10^6$  J/kg and  $L_{\text{ice}}^* = 2.90 \times 10^6$  J/kg which adds a  $\pm 5$  per cent error to estimates of LWC and IWC for the typical range of water contents of clouds with temperatures between  $-40^\circ\text{C}$  and  $0^\circ\text{C}$  (Nevzorov 1983). Therefore, the coefficient  $k$  in Eq. (1) was assumed to be  $k = L_{\text{ice}}^*/L_{\text{liq}}^* \approx 1.12$ .

During the processing of the Nevzorov probe data, the artificial baseline biases of  $W_{\text{TWC}}$  and  $W_{\text{LWC}}$  resulting from changes in the aircraft's true air speed and altitude (Korolev *et al.* 1998) were removed with the help of special software, using complementary information from PMS FSSP, OAP-2DC, OAP-2DP and RICE probes.

### (b) Residual-ice effect

The residual effect of ice on the LWC sensor is related to the small amount of heat removed from the LWC sensor during collisions with ice particles. Figure 1 shows measurements of Nevzorov and RICE probes in a presumably glaciated portion of cloud between 20:25:45 UTC and 20:27:50 UTC. For this period of time the RICE signal  $V_{\text{RICE}}$  is decreasing, meaning that the amount of ice on the surface of the RICE cylinder is decreasing as a result of sublimation caused by adiabatic heating (Mazin *et al.* 2001). If liquid water exists in this cloud, it must be in quantities less than a threshold sensitivity limited by the ice sublimation, estimated theoretically as  $0.006 \text{ g m}^{-3}$  at  $100 \text{ m s}^{-1}$  (Mazin *et al.* 2001). The threshold sensitivity for the RICE probe deduced from in situ measurements was estimated as  $0.01 \text{ g m}^{-3}$  for a 30-second averaging time interval (Cober *et al.* 2001a). As seen from Fig. 1, for a considerable period, the liquid-water content measured by the Nevzorov LWC sensor varies from  $0.01 \text{ g m}^{-3}$  to  $0.08 \text{ g m}^{-3}$

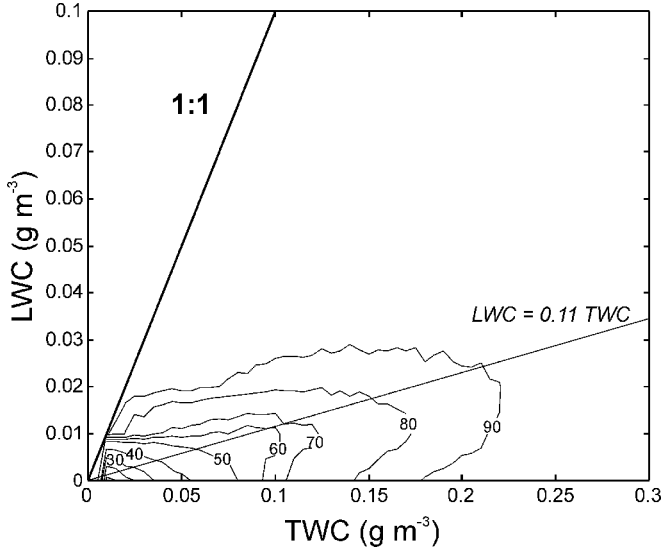


Figure 2. Scatter diagram of liquid-water content (LWC) versus total-water content (TWC) measured by the Nevzorov probe in glaciated clouds, with observation points suppressed for clarity. Contours are isopleths of the percentage probability of finding particular paired values of LWC and TWC inside the contour. Thus, for example, half of all the observed simultaneous values of LWC and TWC lie between the 40 per cent and 90 per cent isopleths.

and exceeds the sensitivity threshold of the RICE. This demonstrates the residual effect of ice on the Nevzorov LWC sensor.

The residual effect of ice may be different in different clouds. The possible reasons for this may be differences in the size, habits and bulk density of particles. The residual effect increases with  $U$  and may reach up to 50 per cent of the indicated ice-content at  $U > 200 \text{ m s}^{-1}$  (Strapp *et al.* 1999). The residual effect of the ice also depends on the sensor temperature. The higher the sensor temperature, the greater the heat exchange between ice particles, and hence the larger residual effect.

The residual-ice effect on the LWC sensor for the dataset in this paper was estimated from the scatter plot (Fig. 2) of  $W_{\text{LWC}}$  versus  $W_{\text{TWC}}$  in glaciated clouds. The clouds were identified as glaciated if  $W_{\text{TWC}}$  exceeded some small threshold value  $W_{\text{thresh}}$  and the response of the RICE probe  $V_{\text{RICE}}$  was not increasing, i.e.

$$W_{\text{TWC}} > W_{\text{thresh}} \quad (7)$$

$$dV_{\text{RICE}}/dt \leq 0. \quad (8)$$

For this study the threshold value was set at  $W_{\text{thresh}} = 0.01 \text{ g m}^{-3}$ . For lower values of  $W_{\text{thresh}}$ , phase discrimination was considered less accurate (because of baseline uncertainty), and, therefore, these cloud regions were disregarded. The best-fit linear regression for the scatter diagram of Fig. 2 gives  $W_{\text{LWC}} = 0.11 W_{\text{TWC}}$  (i.e.  $\beta = 0.11$  in Eq. (2)). Cober *et al.* (2001b), using 30-second averaged data from mostly the same dataset, found similar results.

Note that some cloud regions identified as glaciated, having satisfied the condition of Eq. (8), might still contain some LWC superimposed on the residual effect of ice. The modern conventional technique does not allow separate measurements of LWC and IWC in mixed clouds with an accuracy better than  $0.01 \text{ g m}^{-3}$ . The RICE probe may be insensitive to narrow regions of liquid water even in excess of its threshold sensitivity of

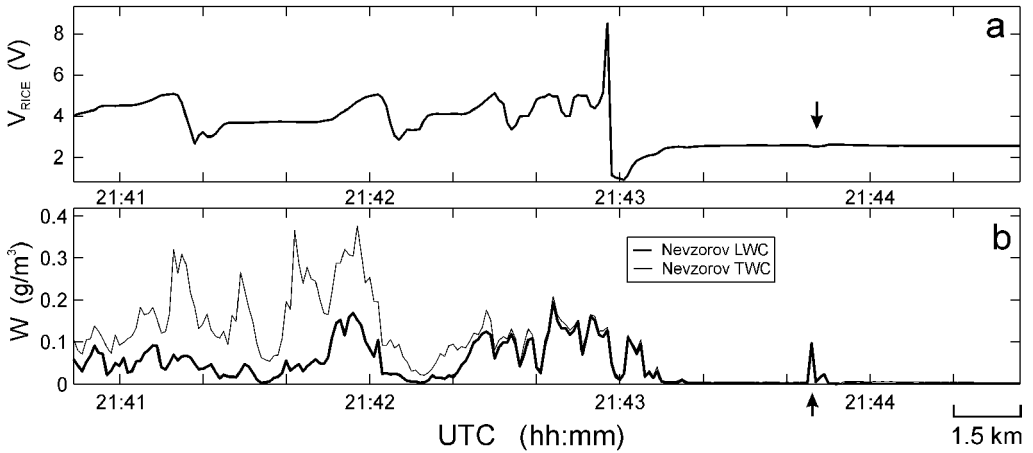


Figure 3. Example when the Rosemount ice detector (RICE) probe may not have responded to the liquid zone's having liquid-water content (LWC) significantly higher than the RICE probe sensitivity threshold. The indicated liquid zone is located at UTC 21:43:45. (a) RICE probe signal and (b) LWC and total-water content (TWC) measured by the Nevzorov probe. Third Canadian Freezing Drizzle Experiment (CFDE3), Ottawa, 9 January 1998, Altostratus/Nimbostratus,  $T = -21$  °C;  $H = 5200$  m.

$0.01 \text{ g m}^{-3}$ . Such an example is shown in Fig. 3, where the RICE probe did not respond to a cloud with a LWC peak up to  $0.1 \text{ g m}^{-3}$  at 21:43:45 UTC. This is probably related to the way in which the RICE responds to the transition from clear sky to a cloud. Many other observations provide evidence that the RICE signal decreases before it increases in the presences of supercooled LWC. If the time in cloud is too short (less than one or two seconds), then the average resulting signal will be negative and close to zero. In addition, the RICE probe does not measure liquid water content but rather the mass of accumulated ice, which to a first approximation is an integral of LWC along the flight track, i.e.  $m = S_{\text{RICE}} \int W_{\text{liq}}(x) dx$ , where  $S_{\text{RICE}}$  is the RICE sample area and  $x$  is the distance along the flight. It may happen that for a narrow cloud with relatively high LWC, the accumulated mass of ice,  $m$ , is still less than the threshold sensitivity of the probe.

### (c) The effect of collection efficiency

In this study, the collection efficiencies  $\varepsilon_{\text{liqT}}$ ,  $\varepsilon_{\text{iceT}}$  and  $\varepsilon_{\text{liqL}}$ , for both LWC and TWC sensors in Eqs. (1) and (2), were assumed to be equal to unity. For most liquid clouds without drizzle-size droplets, the integrated collection efficiency for the LWC sensor  $\varepsilon_{\text{liqL}}$  varies from 0.9 to 1 (Nevzorov 1983; Korolev *et al.* 1998). However, the liquid-water content measured by the TWC sensor may be less than that measured by the LWC sensor up to 20–30 per cent in small droplet clouds ( $D < 5 \mu\text{m}$ ), due to the reduced TWC sensor collection efficiency  $\varepsilon_{\text{liqT}}$ . Such cases, when  $W_{\text{LWC}} > W_{\text{TWC}}$ , were identified as liquid with  $W_{\text{liq}} = W_{\text{LWC}}$  and  $W_{\text{ice}} = 0$ .

The PMS King probe has a significantly reduced efficiency for droplets in the drizzle and rain size range  $MVD > 50 \mu\text{m}$  (Biter *et al.* 1987; Strapp *et al.* 2002). Since the dimensions of the Nevzorov LWC sensor are about the same as those of the PMS King probe, the collection efficiency for the Nevzorov LWC sensor in drizzle is approximately the same as that of the King probe (Strapp *et al.* 2002). However, the collection efficiency of the Nevzorov TWC sensor for drizzle-size droplets is close to unity, as was demonstrated in wind tunnel testing at the NASA Icing Research Tunnel

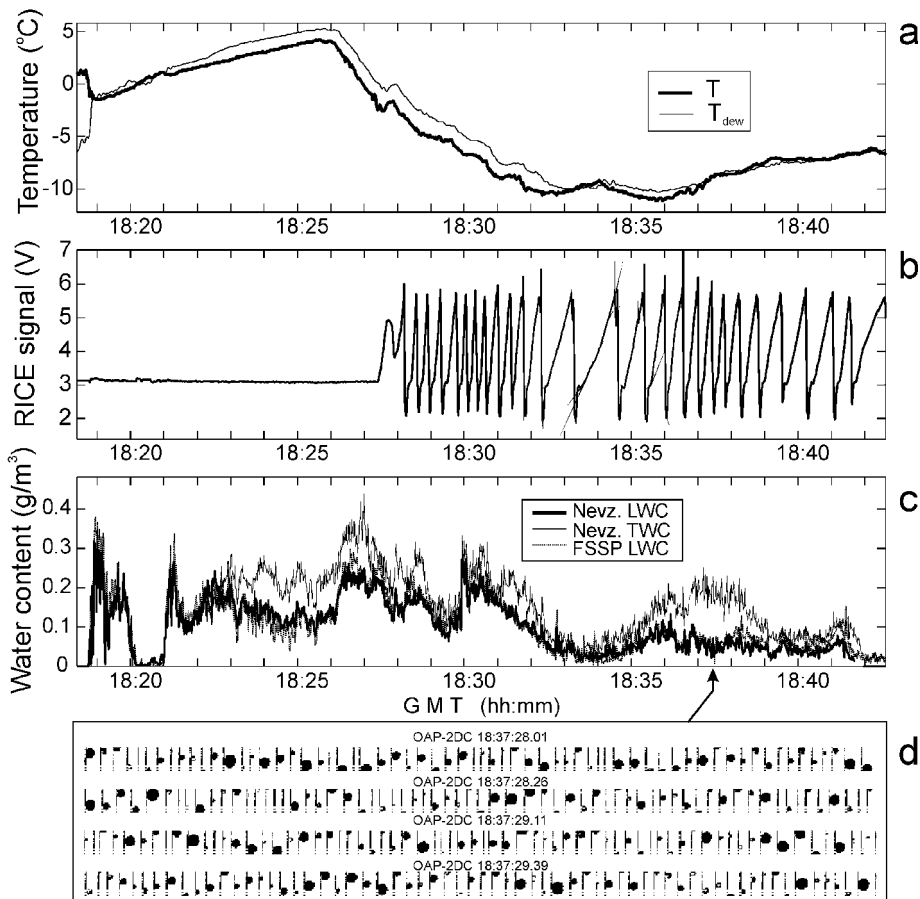


Figure 4. Response of liquid-water content (LWC) and total-water content (TWC) Nevzorov sensors for a liquid cloud containing drizzle: (a) air and dew point temperatures; (b) Rosemount ice detector (RICE) signal; (c) LWC and TWC and (d) an example of 2-D images of drizzle measured by OAP-2DC. First Canadian Freezing Drizzle Experiment (CFDE1), Newfoundland, 9 March 1995,  $H = 450$  m.

(Strapp *et al.* 2002). The difference between the collection efficiencies of the LWC and TWC sensors in drizzling clouds may result in  $W_{TWC}$  being larger than  $W_{LWC}$  by a factor of two (Korolev *et al.* 1998). Such cases may be misinterpreted as mixed phase. To avoid this type of error, cloud regions with all OAP-2DC images with  $D > 100 \mu\text{m}$  being circular (Fig. 4) were segregated and treated differently. The OAP-2DC images were classified using a specially developed habit-recognition algorithm (Korolev and Sussman 2000). The drizzle regions without ice particles were considered as liquid regions, with  $W_{liq} = W_{TWC}$  and  $W_{ice} = 0$ .

#### 4. DESCRIPTION OF THE DATASET

The data on mixed-phase clouds were collected during five field-campaigns: the Beaufort Arctic Storm Experiment (BASE) in September and October 1994, the First Canadian Freezing Drizzle Experiment (CFDE I) in March 1995, the Third Canadian Freezing Drizzle Experiment (CFDE III) December 1997–February 1998, FIRE.ACE in April 1998, and Alliance Icing Research Study (AIRS) December 1999–February

TABLE 1. CHARACTERISTICS OF FLIGHT PROJECTS

Project name	Date	Flight region	Number of flights	In-cloud path length (km)	Main air mass type
BASE	Sept.–Oct. 1994	57°N–74°N; 113°W–141°W	12	3307	Arctic, Continental
CFDE I	March 1995	45°N–53°N; 54°W–63°W	12	9332	Maritime
CFDE III	Dec. 1997–Feb. 1998	42°N–50°N 71°W–83°W	27	17 424	Continental
FIRE.ACE	April 1998	68°N–76°N 133°W–167°W	17	1305	Arctic
AIRS	Dec. 1999–Feb. 2000	42°N–46°N 74°W–82°W	25	12 648	Continental

TABLE 2. LENGTH (km) OF IN-CLOUD MEASUREMENTS DURING DIFFERENT PROJECTS WITH  $TWC > 0.001 \text{ g m}^{-3}$  FOR DIFFERENT TEMPERATURE INTERVALS

	$-35 < T < -30^\circ \text{C}$	$-30 < T < -25^\circ \text{C}$	$-25 < T < -20^\circ \text{C}$	$-20 < T < -15^\circ \text{C}$	$-15 < T < -10^\circ \text{C}$	$-10 < T < -5^\circ \text{C}$	$-5 < T < 0^\circ \text{C}$
BASE	8	360	307	285	498	921	857
FIRE.ACE	84	38	238	362	251	213	18
CFDE1	17	165	380	263	765	2528	3910
CFDE3	0	195	590	1493	2612	5177	6295
AIRS	68	644	628	1479	2410	4787	1931
All Projects	177	1402	2143	3882	6536	13626	13011

2000. The number of NRC Convair 580 flights included in the analysis, the type of air mass, and the region of the flights are indicated in Table 1. The duration of the NRC Convair 580 flights was typically between 2 and 5 hours.

The bulk of the data was collected in stratiform clouds (*St*, *Sc*, *Ns*, *As*, *Ac*), usually associated with frontal systems. During the BASE and FIRE.ACE projects, a number of flights sampled cirrus clouds. The scale of spatial averaging is about 100 m (1 s). The total flight length in cloud with  $W_{TWC} > 0.01 \text{ g m}^{-3}$  was 44 013 km. The temperature and altitude of measurements ranged from  $0^\circ \text{C}$  to  $-35^\circ \text{C}$  and from 0 km to 6 km, respectively. The frequency of occurrence of different parameters associated with the analysis of the phase composition of clouds was calculated for seven 5 degC intervals in the range  $0^\circ \text{C}$  to  $-35^\circ \text{C}$ . Table 2 shows the length of the in-cloud legs for different temperature intervals having  $W_{TWC} > 0.01 \text{ g m}^{-3}$  to estimate the significance of the statistics on the mixed phase presented below. As seen from Table 2, most of the data were collected at temperatures in the range  $-15^\circ \text{C} < T < 0^\circ \text{C}$ .

## 5. EXPERIMENTAL RESULTS

### (a) Definition of a cloud phase-composition

The phase composition was characterized with the help of a phase-composition coefficient,  $\mu_n$  (Korolev 1998)

$$\mu = \frac{\sum_j \alpha_{ice j} N_{ice j} D_{ice j}^n}{\sum_j \alpha_{ice j} N_{ice j} D_{ice j}^n + \sum_i \alpha_{liq j} N_{liq i} D_{liq i}^n} = \frac{\overline{\alpha_{ice} N_{ice} D_{ice}^n}}{\overline{\alpha_{ice} N_{ice} D_{ice}^n} + \overline{\alpha_{liq} N_{liq} D_{liq}^n}}. \quad (9)$$

Here  $N_{liq}$  and  $N_{ice}$  are the number concentration of liquid droplets and ice particles, respectively;  $D_{liq}$  and  $D_{ice}$  are the droplet diameter, and characteristic size of ice particles,

respectively;  $n = 0, 1, 2, 3 \dots$  is the moment of the phase-composition coefficient;  $\overline{\alpha_{ice}}, \overline{\alpha_{liq}}$  are the coefficients dependent on the moment  $n$ . For example  $\overline{\alpha_{ice}}, \overline{\alpha_{liq}}$  are equal to the extinction efficiency for  $n = 2$ , or bulk density for  $n = 3$ . The advantage of  $\mu_n$  is that it changes in a limited interval, i.e. from  $\mu_n = 0$ , when the cloud is completely liquid, to  $\mu_n = 1$ , when the cloud is completely glaciated.

Within the cloud physics community there is no clear definition of ‘liquid’, ‘mixed’ and ‘ice’ (or ‘glaciated’) cloud. For example, should a cloud be defined as mixed, if it has one ice particle per  $10^1$  or per  $10^{100}$  droplets? Should a cloud be considered glaciated if it contains one liquid droplet per  $10^{100}$  ice particles, or is it still mixed? What moments  $n$  of the phase-composition coefficient  $\mu_n$  should be used for the definition of liquid and ice clouds? Such a definition should probably depend on the problem being solved. Thus,  $\mu_6$  should probably relate to radar studies, while radiative transfer models and lidar sensing might consider  $\mu_2$ .

Since we are considering cloud-water content, the cloud phase-composition will be characterized by the phase-composition coefficient of the third moment, i.e.

$$\mu_3 = \frac{\overline{\rho_{ice} N_{ice} D_{ice}^3}}{\overline{\rho_{ice} N_{ice} D_{ice}^3} + \overline{\rho_{liq} N_{liq} D_{liq}^3}} \cong \frac{W_{ice}}{W_{ice} + W_{liq}}. \quad (10)$$

The phase-composition coefficient used in this study is similar to the ‘fractional ice content’ of Tremblay *et al.* (1996). Some other authors have used ‘liquid-water fraction’ ( $1 - \mu_3$ ) to describe the mixed-phase composition of clouds (e.g. Moss and Johnson 1994).

Because of instrument limitations, the value of  $\mu_3$  cannot be resolved to an accuracy better than about 0.1. Consequently, clouds with  $\mu_3 < 0.1$  will be defined as liquid; clouds with  $0.1 \leq \mu_3 \leq 0.9$  as mixed; and clouds having  $\mu_3 > 0.9$  as glaciated or ice clouds. It should be emphasized that these definitions of liquid and ice clouds are motivated by limited instrument resolution, rather than by physical concepts. Therefore, the clouds defined as liquid may still contain a small fraction of ice, and ice clouds may contain some liquid droplets. Nevertheless, using these definitions, results can be obtained that are useful for theoretical and applied cloud physics.

### (b) *Mixed-phase composition versus temperature*

Figures 5(a,b) show the frequency and cumulative distributions of  $\mu_3$  in seven 5 degC intervals in the range  $-35^\circ\text{C} < T < 0^\circ\text{C}$ . The curves in Fig. 5(a) show explicit minima in the range  $0.1 < \mu_3 < 0.9$  for all temperature intervals. At the same time, there are two explicit maxima: one for  $\mu_3 < 0.1$  (liquid clouds) and another one for  $\mu_3 > 0.9$  (ice clouds). The fraction of liquid clouds ( $\mu_3 < 0.1$ ) decreases with decreasing temperature from about 50 per cent for  $-5^\circ\text{C} < T < 0^\circ\text{C}$  down to 5 per cent for  $-35^\circ\text{C} < T < -30^\circ\text{C}$ . However, the fraction of glaciated clouds increases with decreasing temperature from 20 per cent for  $-5^\circ\text{C} < T < 0^\circ\text{C}$  up to 50 per cent for  $-35^\circ\text{C} < T < -30^\circ\text{C}$ . The frequency of occurrence of mixed-phase clouds stays approximately constant in the range  $0.2 < \mu_3 < 0.5$ . An increase of the threshold,  $W_{\text{thresh}}$ , results in a decrease of the fraction of glaciated clouds and an increase of the fraction of liquid clouds, whereas the shape of the density distributions of  $\mu_3$  stays about the same as in Fig. 5(a).

It should be mentioned that although the data were collected during different flight campaigns there are some differences in the distributions of  $\mu_3$  for each specific project compared with that shown in Fig. 5. These are related to regional differences and

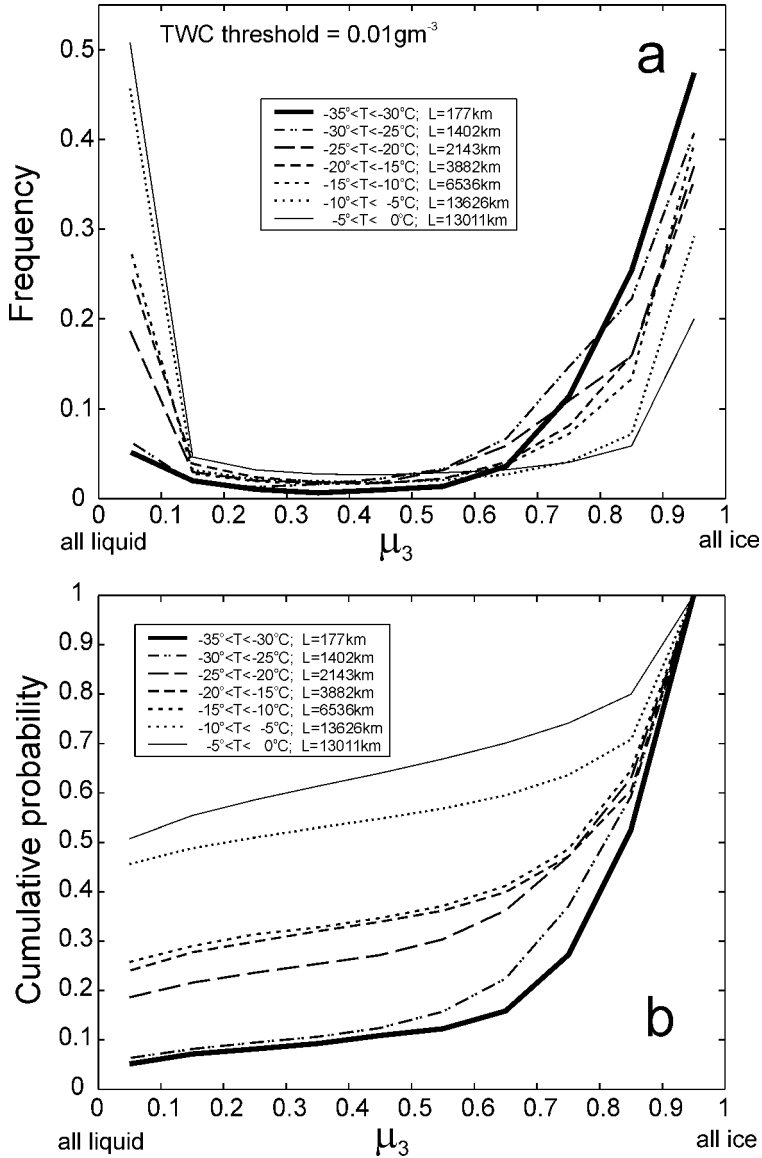


Figure 5. Probability distributions of mixed-phase composition coefficient  $\mu_3$  for different temperature intervals: (a) density and (b) cumulative.  $\mu_3 = 0$  in liquid clouds;  $\mu_3 = 1$  in ice clouds.

differences in characteristic flight temperatures and altitudes. However, the tendency for the frequency of occurrence of  $\mu_3$  to reach a minimum in the range of  $0.2 < \mu_3 < 0.5$ , and maxima at  $\mu_3 < 0.1$  and  $\mu_3 > 0.9$  remains the same.

(c) *Relation between mixed-phase composition and water content*

Figures 6(a,b,c) show the dependence of the average IWC, LWC and TWC on temperature for differing  $\mu_3$ . The lowest curve in Fig. 6(a) shows IWC in liquid clouds ( $\mu_3 < 0.1$ ) staying approximately constant for all temperature intervals and equal to approximately  $0.002 \text{ g m}^{-3}$ , which is much less than  $W_{\text{thresh}}$ . This provides support for

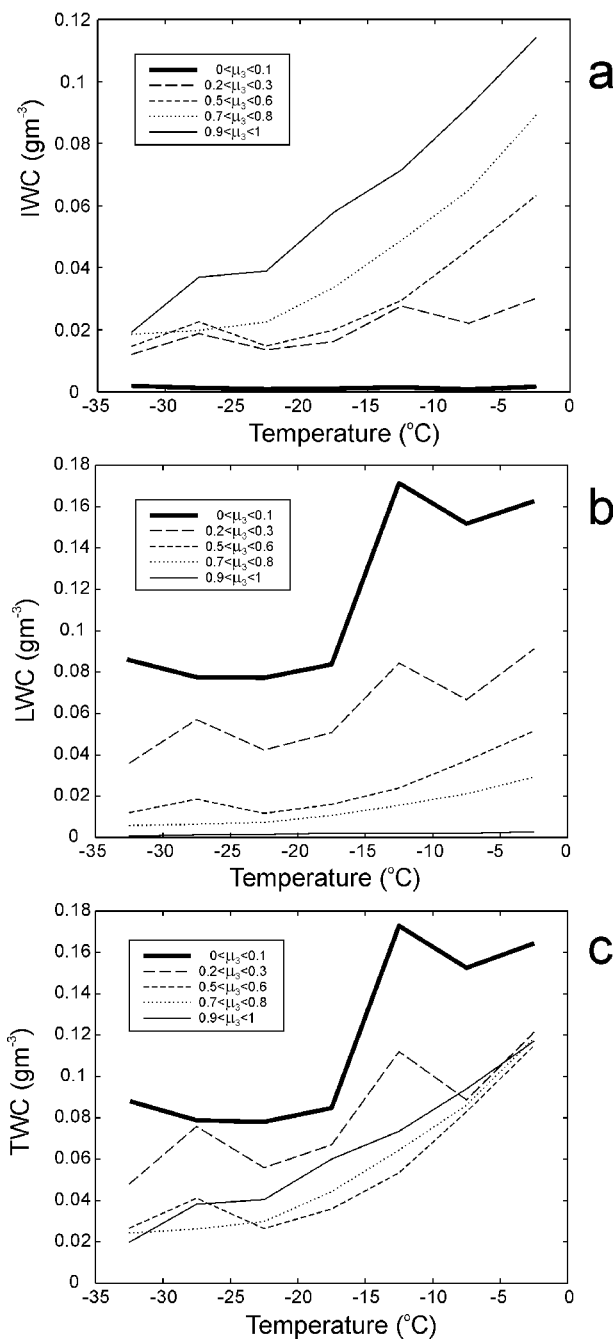


Figure 6. Values of water content versus temperature for different values of phase composition coefficient  $\mu_3$ : (a) ice-water content (IWC); (b) liquid-water content (LWC) and (c) total-water content (TWC).

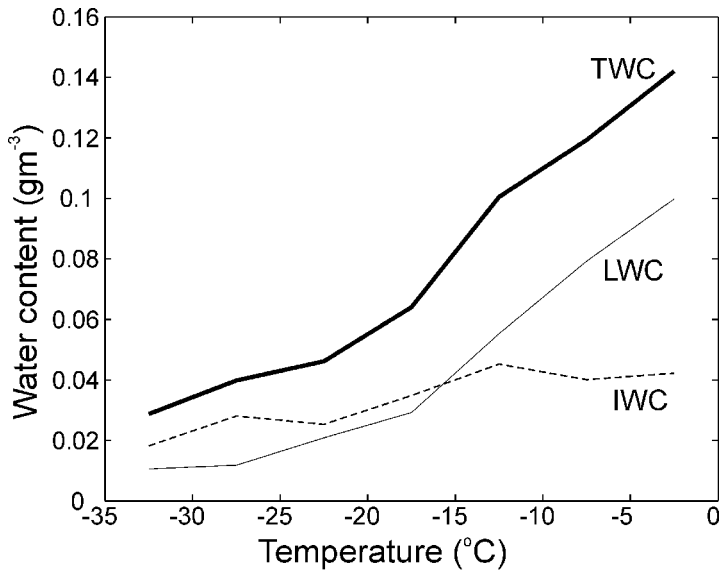


Figure 7. Dependence of ice-water content (IWC), liquid-water content (LWC) and total-water content (TWC) on temperature, averaged over clouds having all types of phase composition.

the method of correcting the residual effect of ice for the LWC sensor, since the IWC in liquid clouds should be close to zero. The highest curve in Fig. 6(a) shows IWC in ice clouds ( $\mu_3 > 0.9$ ). The other curves demonstrate the behaviour of IWC versus  $T$  in mixed-phase clouds having different values of  $\mu_3$ . As seen from Fig. 6(a), IWC on average decreases with decreasing temperature for all values of  $\mu_3$ .

Figure 6(b) shows the dependence of LWC on temperature for differing  $\mu_3$ . Behaving in much the same way as IWC, LWC on average decreases with temperature. An increase of LWC in liquid clouds (top curve in Fig. 6(b)) at  $-35^\circ\text{C}$  may be related to poor statistics, since the total in-cloud length associated with this point is only about 12 km.

Figure 6(c) shows the dependence of TWC on temperature. Basically it can be obtained by summing the curves corresponding to same values of  $\mu_3$  in Figs. 6(a,b). TWC in mixed-phase clouds with  $0.5 < \mu_3 < 0.8$  is lower than liquid ( $\mu_3 < 0.1$ ) and ice ( $\mu_3 > 0.9$ ) clouds in all temperature intervals.

Figure 7 shows the dependence of IWC, LWC and TWC on temperature for the whole range of  $\mu_3$ , i.e. in all clouds regardless of their phase composition. As seen from Fig. 7, IWC, LWC and TWC monotonically decrease from 0.04 to 0.02  $\text{g m}^{-3}$ , from 0.1 to 0.01  $\text{g m}^{-3}$ , and from 0.14 to 0.03  $\text{g m}^{-3}$ , respectively, when the temperature decreases from  $0^\circ\text{C}$  to  $-35^\circ\text{C}$ . Note that IWC does not change as much as LWC and stays nearly constant.

#### (d) Relation between mixed-phase composition and cloud-particle concentration

Recent studies have implied that FSSP measurements can be used for estimation of cloud particle number-concentration in mixed and ice clouds (Gayet *et al.* 1996; Arnott *et al.* 2000; Ivanova *et al.* 2001). Problems could arise from particle impaction and possible shatter of larger particles on surfaces upstream from the sensor, particularly for larger particles and for flow at an angle to the housing. In the studies reported here, the concentration of larger particles capable of shatter (Gardiner and Hallett 1985;

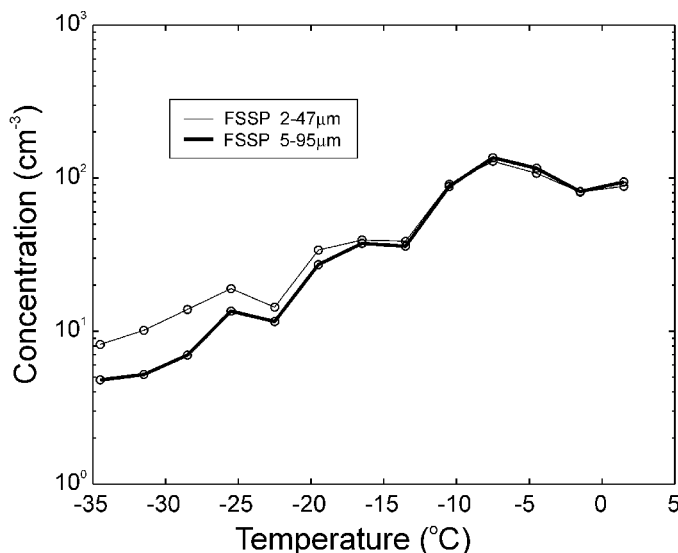


Figure 8. Concentration of cloud particles ( $\text{cm}^{-3}$ ) versus temperature averaged over all projects. The concentration was measured by two forward-scattering spectrometer probes (FSSPs) in characteristic diameter ranges 2–32  $\mu\text{m}$  (or 2–47  $\mu\text{m}$ ) and 5–95  $\mu\text{m}$ .

Hallett and Isaac 2002) appears not to be significant and the numbers of ice particles given over the range of the two FSSPs was taken as the ice concentration. *In situ* measurements conducted in ice clouds with replicators and optical spectrometers show that ice particles  $D > 50 \mu\text{m}$  is often one to three orders of magnitude less than smaller particles  $D < 50 \mu\text{m}$  (Heymsfield and Platt 1984; Pueschel *et al.* 1997). Therefore, it is expected that the shattering of large crystals would not affect significantly the measured concentration of cloud particles. Nevertheless, it is acknowledged that the use of the FSSP to measure ice-particle concentration remains a matter of debate. In the following sections, the FSSP probe is used to estimate ice concentrations in mixed and glaciated clouds.

Figure 8 shows a comparison of average particle-number concentration  $N_1$  and  $N_2$  measured by two FSSPs operated in different size ranges of 2  $\mu\text{m}$  to 32  $\mu\text{m}$  or 3  $\mu\text{m}$  to 45  $\mu\text{m}$  (FSSP#96) and 5  $\mu\text{m}$  to 95  $\mu\text{m}$  (FSSP#124), respectively. As seen from Fig. 8, the concentration  $N_1$  agrees to within 5 per cent to 10 per cent of  $N_2$  at temperatures  $T > -20 \text{ }^\circ\text{C}$ . The FSSP size-bin thresholds are calibrated for liquid droplets; therefore the measurements of two FSSPs in clouds dominated by droplets are expected to agree in both size-ranges. The concentration of droplets at these temperatures on average exceeds that of ice particles. As a consequence, the concentration of ice does not significantly affect the total concentration. At lower temperatures,  $T < -20 \text{ }^\circ\text{C}$ , when the average concentration of ice particles becomes dominant, the difference between  $N_1$  and  $N_2$  reaches a factor of two. Such a difference may be due to different FSSP response to ice in different size-ranges. In general, the concentration of cloud particles decreases with decreasing temperature.

Figure 9 shows cloud-particle concentration  $N_1$  (Fig. 9(a)) and  $N_2$  (Fig. 9(b)) versus  $\mu_3$  in different temperature intervals. As seen, the concentration monotonically decreases towards  $\mu_3 = 1$  (ice clouds) to approximately the same limit in all temperature ranges.

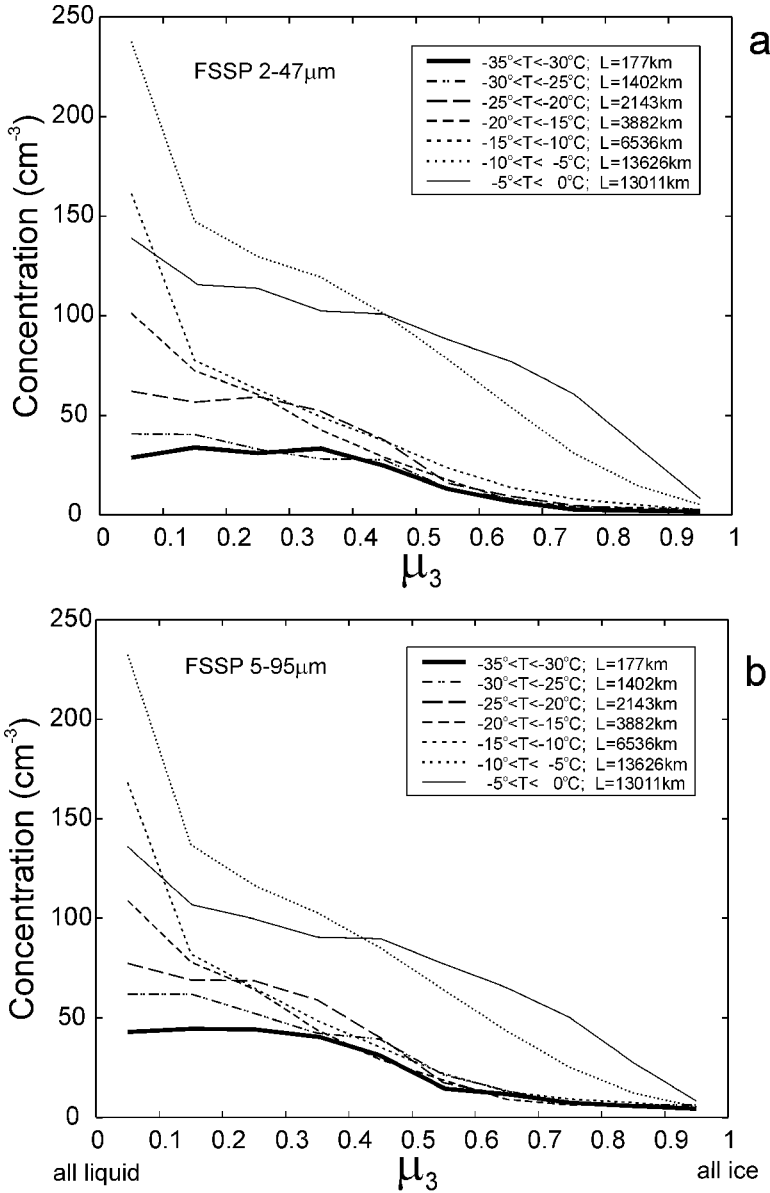


Figure 9. Average concentration of cloud particles ( $\text{cm}^{-3}$ ) versus  $\mu_3$  for different temperature intervals. The concentration was measured by two forward-scattering spectrometer probes (FSSPs) in characteristic diameter ranges 2–32  $\mu\text{m}$  or 2–47  $\mu\text{m}$  (a) and 5–95  $\mu\text{m}$  (b). Phase composition coefficient  $\mu_3 = 0$  in liquid clouds and  $\mu_3 = 1$  in ice clouds.

Figure 10 shows the dependence of the cloud-particle concentration  $N_1$  (Fig. 10(a)) and  $N_2$  (Fig. 10(b)) versus temperature for different ranges of  $\mu_3$ . Figure 10 indicates that the concentration monotonically decreases with decreasing of temperature for all values of  $\mu_3$ . The most interesting observation is that the particle concentration stays approximately constant at  $T < -10^\circ\text{C}$  in ice clouds ( $\mu_3 > 0.9$ ). Below  $-10^\circ\text{C}$  the value of  $N_1$  varies somewhat between  $2 \text{ cm}^{-3}$  and  $3 \text{ cm}^{-3}$ , and the concentration  $N_2$

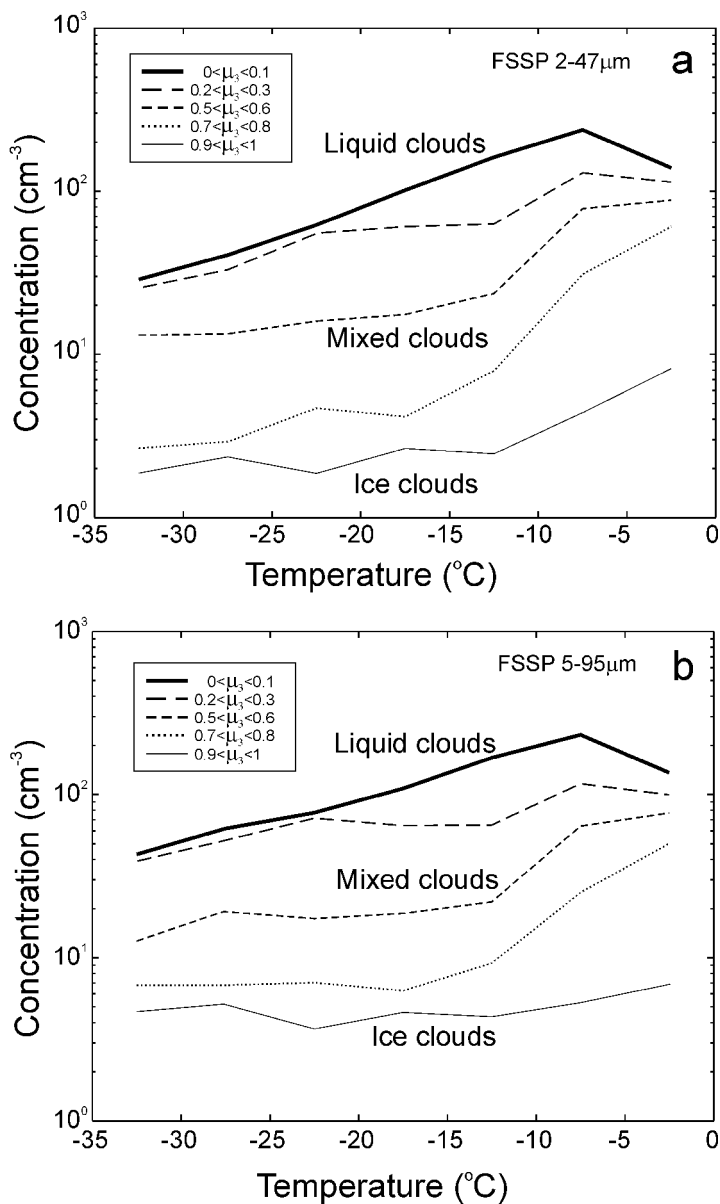


Figure 10. Average concentration of cloud particles versus temperature for different values of the phase composition coefficient  $\mu_3$ . The concentration was measured by two forward-scattering spectrometer probes (FSSPs) in the characteristic diameter ranges (a) 2–32  $\mu\text{m}$  or 2–47  $\mu\text{m}$  and (b) 5–95  $\mu\text{m}$ .

varies between  $5 \text{ cm}^{-3}$  and  $6 \text{ cm}^{-3}$ . This concentration may be interpreted as an estimate of the concentration of ice particles. An increase of  $N_1$  and  $N_2$  at  $T > -10 \text{ }^\circ\text{C}$  may be explained by the presence of a small fraction of liquid droplets.

The apparent lack of dependence of ice-particle concentration on temperature is an interesting observation requiring further explanation. This observation is in agreement with the previous studies of Korolev *et al.* (2000), Gultepe *et al.* (2001) and Field *et al.* (2002).

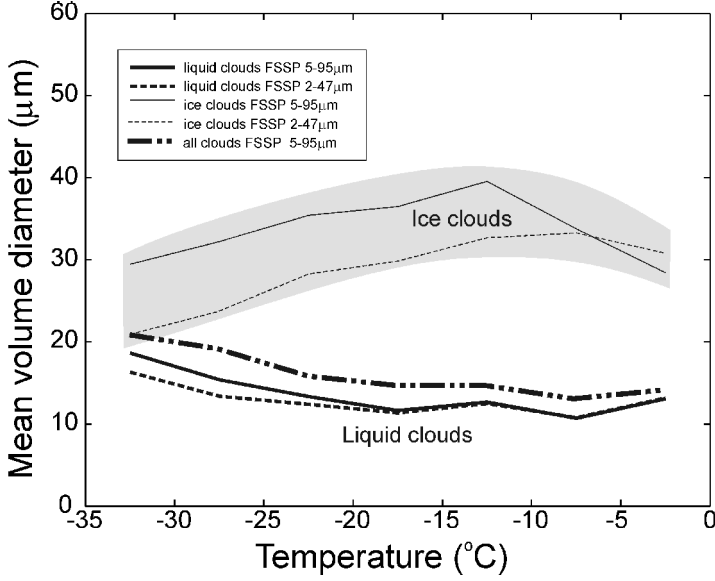


Figure 11. Average mean-volume diameter of cloud particles versus temperature for liquid clouds, ice clouds and all clouds, derived from measurements by the Nevzorov and forward-scattering spectrometer probes.

(e) *Mean volume diameter of cloud particles in ice and liquid clouds*

Measurements of particle number concentration and their mass enable an estimate of mean-volume diameter of cloud particles, viz.

$$\overline{D}_3 = \left( \frac{6W}{\pi\rho N} \right)^{1/3}. \quad (11)$$

Here  $W$  is cloud water content measured by the Nevzorov probe;  $N$  is the concentration measured by the FSSP; and  $\rho$  is the density of the cloud particles.

Figure 11 shows the dependence of  $\overline{D}_3$  on temperature for ice ( $\mu_3 > 0.9$ ) and liquid clouds ( $\mu_3 < 0.1$ ). The mean-volume diameter in liquid clouds slightly increases with decreasing temperature from about 12  $\mu\text{m}$  to 18  $\mu\text{m}$ . In ice clouds  $\overline{D}_3$  varies from approximately 20  $\mu\text{m}$  to 35  $\mu\text{m}$ . As seen from Fig. 11,  $\overline{D}_3$  has a maximum in the temperature range of  $-15^\circ\text{C} < T < -10^\circ\text{C}$ , which is consistent with the temperature range of the maximum diffusional growth rate of ice. Mean-volume diameters calculated for all clouds are rather close to  $\overline{D}_3$  in liquid clouds, increasing from about 15  $\mu\text{m}$  to 20  $\mu\text{m}$  with decreasing temperature (Fig. 11).

The density of ice particles in the atmosphere varies from about 50  $\text{kg m}^{-3}$  for crystal arrays to 920  $\text{kg m}^{-3}$  for solid ice, depending on particle size and habit (e.g. Heymsfield 1972; Ryan *et al.* 1976). The density of ice particles increases with decreasing particle-size, approaching 920  $\text{kg m}^{-3}$  for small ice particles. The mean-volume size of ice particles, as shown in Fig. 11, was calculated with an ice density of  $\rho = 800 \text{ kg m}^3$ . Such an assumption may be justified by the small characteristic sizes of ice particles found in this study. It is worth noting, that since  $\rho$  in Eq. (11) is raised to  $-1/3$  power, a decrease of the density of ice by a factor of two would result in only a 20 per cent increase of  $\overline{D}_3$ . Therefore, the expected uncertainty in  $\rho$  would not significantly affect the values of  $\overline{D}_3$  shown in Fig. 11.

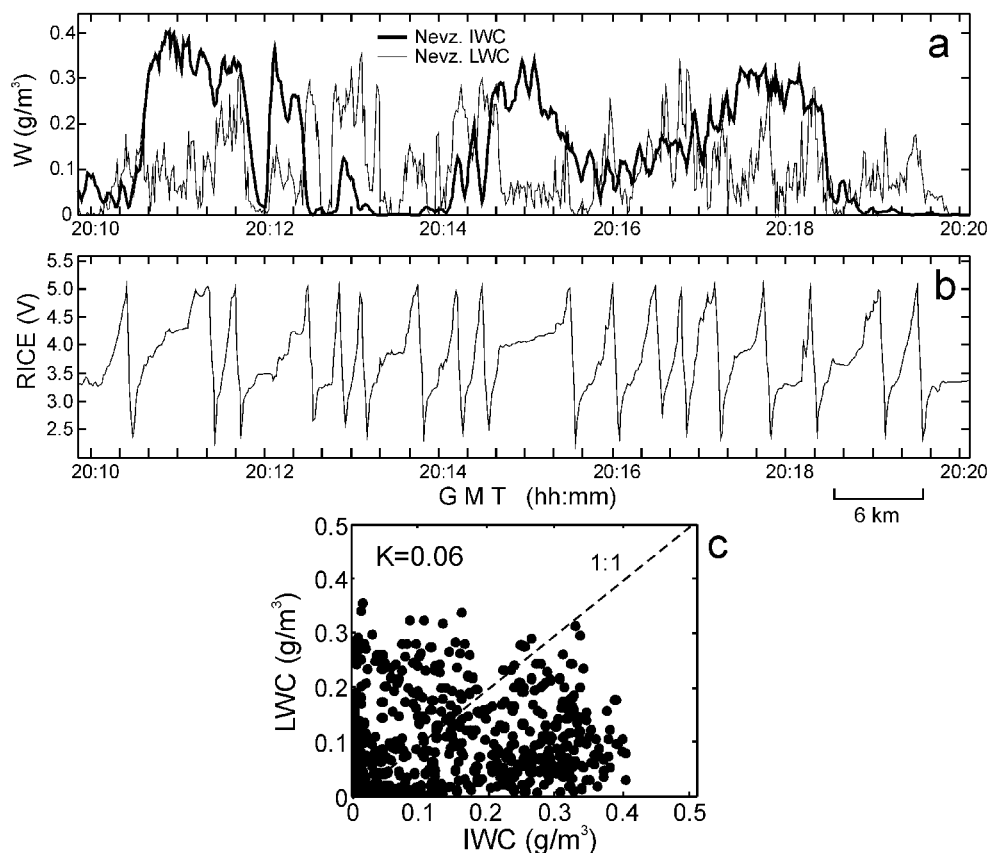


Figure 12. Example of low correlation between liquid-water content (LWC) and ice-water content (IWC): (a) Rosemount ice detector (RICE) signal; (b) liquid-water content (LWC) and ice-water content (IWC) measured by Nevzorov LWC/TWC probe; (c) scatter plot of LWC and IWC. The correlation coefficient between LWC and IWC for the indicated period is 0.06. Alliance Icing Research Study (AIRS), Ottawa, 16 December 1999, Nimbostratus.  $T = -6^\circ\text{C}$ ;  $H = 1200$  m.

### (f) Correlation between LWC and IWC

Analysis of in situ measurements has shown that there is no correlation between IWC and LWC in mixed-phase clouds. An example of simultaneous measurements of LWC and IWC is shown in Fig. 12(a). The scatter plot of LWC and IWC in Fig. 12(c) indicates an absence of any correlation between these parameters. The correlation coefficient between LWC and IWC for this case was found to be  $r = 0.06$ . In general, the correlation coefficient between LWC and IWC varies somewhat between  $-0.3$  and  $0.3$ .

Since the IWC in mixed clouds grows at the expense of LWC, one would expect a high correlation coefficient between these two parameters. However, the absence of a correlation may be explained because the rate of growth of IWC is governed by the supersaturation over ice. The supersaturation in mixed-phase clouds stays constant and nearly equal to the saturation over water before complete evaporation of liquid droplets (Korolev and Isaac 2002a), and therefore it is independent of the current value of LWC. The spatial correlation may be also reduced when glaciation in different cloud regions starts at different times.

## 6. DISCUSSION

(a) *Characteristic size of cloud ice-particles*

The mean-volume diameter of ice particles, as shown in Fig. 11, was found to be rather small. Most numerical models of radiative transfer in clouds have ice particles with characteristic sizes of about a few hundred micrometres. Existing knowledge of the characteristic sizes of ice particles is based mainly on measurements made using OAP-2D imaging probes. Usually, particles having non-circular shapes are considered to be ice. However, OAP-2D probes have a poor image-resolution that does not allow judgments about shape for particles smaller than about 5 pixels in size, equivalent to  $100\ \mu\text{m}$  to  $125\ \mu\text{m}$  at the typical  $25\ \mu\text{m}$  pixel resolution of an OAP-2DC probe. Recent measurements of ice-particle sizes in glaciated clouds using a high image resolution ( $2.3\ \mu\text{m}$ ) cloud-particle imager (CPI) have indicated the presence of a large fraction of small ice-particles in glaciated clouds (Lawson *et al.* 2001). This is consistent with the CPI measurements collected from the NRC Convair 580 during the FIRE.ACE, CFDE III and AIRS projects.

In some glaciated clouds, TWC measured by the Nevzorov probe agrees reasonably well with water content derived from FSSP data, assuming spherical ice-particles with a density of  $900\ \text{kg m}^{-3}$ . Such measurements, unless fortuitous, support the above conclusion that glaciated clouds are mainly composed of small particles, and that concentrations and sizes can be reasonably estimated using the FSSP. If this were not true, the TWC measured by the Nevzorov probe and that derived from FSSP data would disagree significantly. One such case is shown in Fig. 13. The FSSP ice-water content in the range  $5\ \mu\text{m}$  to  $95\ \mu\text{m}$  agrees better with the Nevzorov TWC than with the Nevzorov LWC. One would expect this result if ice particles are small (i.e. fall in the size range  $5\ \mu\text{m}$  to  $95\ \mu\text{m}$ ) and have a compact shape. Analysis of a large dataset of CPI images shows that in glaciated clouds a large fraction of particles with  $d < 60\ \mu\text{m}$  do indeed have a quasi-spherical compact shape (Korolev and Isaac 2002b). It should be noted that cases with agreement such as illustrated in Fig. 13 do not occur all the time. However, it is not a rare situation.

Other evidence regarding the characteristic size of ice particles comes from measurements of the effective diameter of cloud particles. It can be shown that, since this parameter is defined as  $D_{\text{eff}} = \overline{D_3^3} / \overline{D_2^2}$ , for any size distribution the following relationship between various diameter definitions always holds:  $D_{\text{eff}} \geq \overline{D_3} \geq \overline{D_2} \geq \overline{D}$ . Based on an independent large dataset of aircraft data, Korolev *et al.* (2001) showed that the effective diameter stayed approximately constant throughout the temperature range of  $-50\ ^\circ\text{C} < T < 10\ ^\circ\text{C}$ . For the range of  $-50\ ^\circ\text{C} < T < -30\ ^\circ\text{C}$  where all cloud particles were presumably ice,  $D_{\text{eff}}$  was found to be about  $14\ \mu\text{m}$ . These results were obtained with rather simple measurements of TWC and extinction, and were not subject to the controversy of small-ice-particle measurements with an FSSP probe. Their  $D_{\text{eff}}$  results were even lower than the values of  $\overline{D_3}$  shown in Fig. 11. Comparisons of  $\overline{D_3}$  and  $D_{\text{eff}}$  rather suggest that  $\overline{D_3}$  might even be less than that shown in Fig. 11.

Ice particles breaking on impact on the FSSP inlet tube may produce artefacts that erroneously increase concentrations. Plate crystals  $> 200\ \mu\text{m}$  begin to shatter at aircraft speeds above about  $150\ \text{m s}^{-1}$  (Hallett 1976). Thus, although the FSSP may give a good indication of crystal concentration for small sized particles (e.g as in Fig. 13), over-counting may occur in the presence of large ice-particles. However, the comparison of  $\overline{D_3}$  in this study and  $D_{\text{eff}}$  in the study of Korolev *et al.* (2000) provides indirect evidence that the FSSP gives a reasonable estimate of the concentration of ice particles in glaciated clouds.

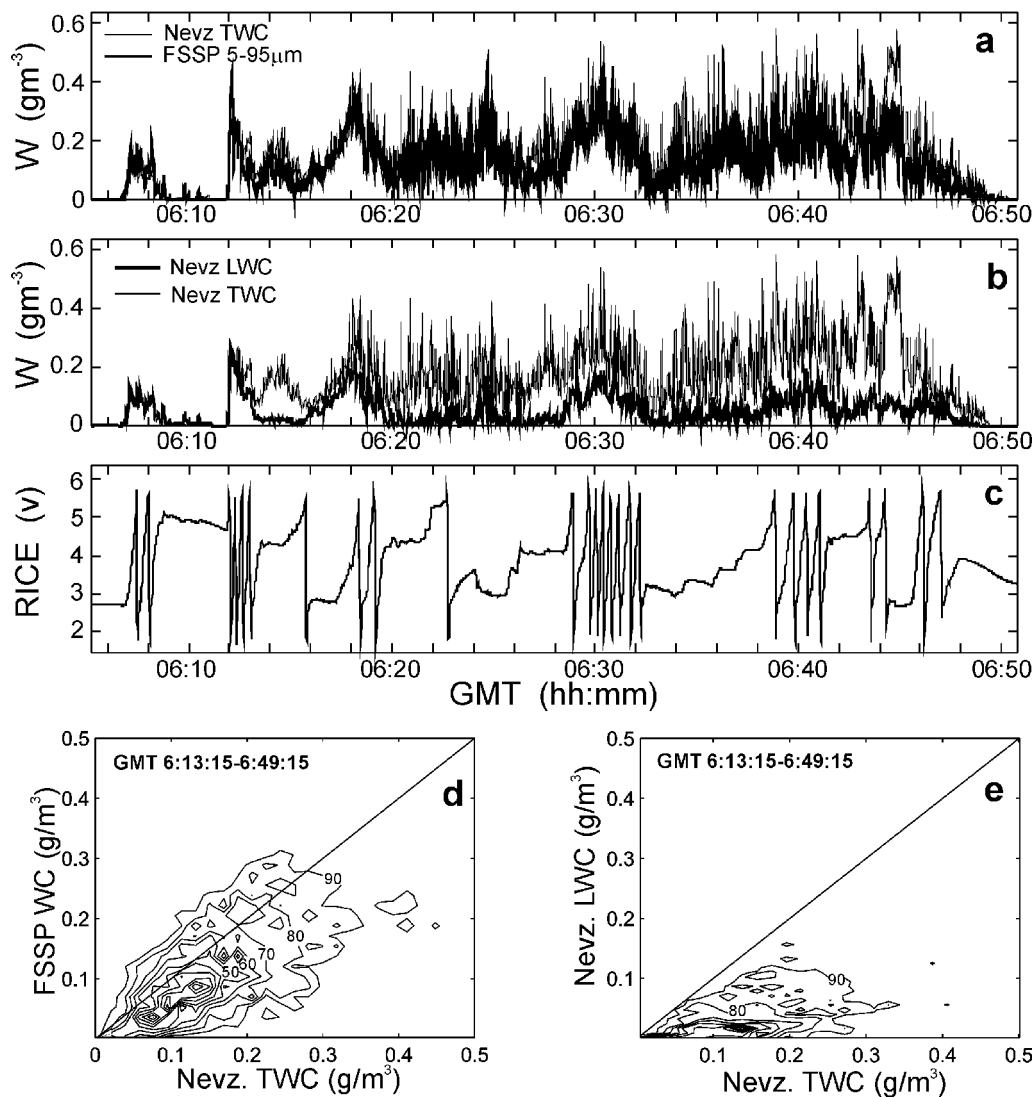


Figure 13. Comparison of water content measurements: (a) total-water content (TWC) by the Nevzorov probe and derived from forward-scattering spectrometer probe (FSSP); (b) liquid-water content (LWC) and TWC by the Nevzorov probe; (c) Rosemount ice detector (RICE) signal; (d) probability isopleths of a scatter plot of Nevzorov TWC and water content derived from FSSP data and (e) probability isopleths of a scatter plot of Nevzorov LWC and Nevzorov TWC. Contours in (d) and (e) are isopleths of percentage probability for finding points with the paired water contents inside the contour. First Canadian Freezing Drizzle Experiment (CFDE1), Newfoundland, 7 March 1995, Nimbostratus,  $T = -1^{\circ}\text{C}$  to  $-8^{\circ}\text{C}$ .

In this study,  $\overline{D_3}$  may be biased by the presence of a small quantity of liquid droplets. They do not affect TWC, but may dominate the particle-number concentration. Such clouds would still fall into the category of glaciated clouds. In this case, in order to get  $\overline{D_3}$  biased by a factor of two,  $N_{\text{ice}}$  should be biased by liquid droplets on average eight times (see Eq. (11)).

(b) *Relation between glaciation and residence time of cloud particles*

The experimental results presented in Fig. 5 show explicit minima of  $\mu_3$  in all temperature intervals. These minima are a result of the instability of mixed-phase clouds. At the same time, the maximum at  $\mu_3 = 1$  indicates that the clouds transit through the mixed-phase stage and convert into ice. This leads to an important conclusion that the glaciation time ( $\tau_{gl}$ ) is usually less than the characteristic residence-time of liquid particles in clouds ( $\tau_{res}$ ), i.e.

$$\tau_{gl} \ll \tau_{res}. \quad (12)$$

If the above inequality were reversed, mainly liquid clouds would be observed and the maximum at  $\mu_3 = 1$  for ice clouds would not be observed. The residence time of cloud particles cannot exceed the lifetime of the cloud, but may be significantly less.

To date, there have been no direct measurements of the residence time of cloud particles. Under some assumptions, it can be estimated theoretically. Korolev and Isaac (2002a) showed that, for  $LWC \approx 0.1 \text{ g m}^{-3}$ ,  $N \approx 10^1 \text{ l}^{-1}$  to  $10^2 \text{ l}^{-1}$ , and  $U_z = 0$ , the characteristic glaciation time is approximately tens of minutes, giving an indirect estimation of  $\tau_{res}$  in stratiform clouds.

(c) *Comparison with previous studies of mixed-phase clouds*

Zak (1937) studied the statistics of phase composition versus temperature in stratiform frontal clouds using an impactor technique. She found that the maximum frequency of occurrence of supercooled water in clouds was about 56 per cent at  $T < -8^\circ\text{C}$ . Then it gradually decreased towards colder temperatures, reaching close to 0 at  $-40^\circ\text{C}$ . Borovikov *et al.* (1963), using nearly 9000 aircraft impactor samples, derived the frequency of occurrence of liquid, mixed, and ice clouds at different temperature intervals (Fig. 14). In their study, an impactor sample was considered to be liquid if it did not contain ice particles, and it was considered as ice if there were no spherical particles that could be identified as droplets. The rest of the samples were assumed to be mixed phase. Such an approach implies that Borovikov *et al.* (1963) defined mixed-phase composition based on number concentration, which is the zero moment of the phase-composition coefficient  $\mu_0$  (section 5(a)).

Mazin *et al.* (1992) and Nevzorov (2000), using a set of instruments including several particle spectrometers, the Nevzorov LWC/TWC probe and a cloud extinction meter, concluded that only a small fraction of clouds are completely liquid or completely glaciated. Most clouds were found to have mixed phase. One of the reasons for such a large difference from the present study is the difference in definitions of ice and liquid clouds (section 5(a)). Another reason may be related to an underestimate of the residual effect of ice on the LWC sensor (see section 3(b)).

Figure 14 shows a comparison of the fraction of ice, mixed and liquid clouds obtained in different studies. The results of Cober *et al.* (2001b) are for a subset (CFDE I and CFDE III experiments) of the same dataset used in this study. Although the present study incorporates a wider dataset with some additional geographical area, the results are quite similar. It should be noted that the studies of Mossop, *et al.* (1970), Isaac and Schemenauer (1979), and Wallace and Hobbs (1975) all refer to the appearance of ice particles on aircraft instruments at different altitudes in convective clouds. Peppler (1940) made his conclusion based on impactor samplings similar to that used by Zak (1937) and Borovikov *et al.* (1963). Moss and Johnson (1994) estimated mixed phase from OAP-2DC and Johnson–Williams liquid-water-probe measurements. Figure 14 gives some idea about how different definitions, instruments, and geographical location

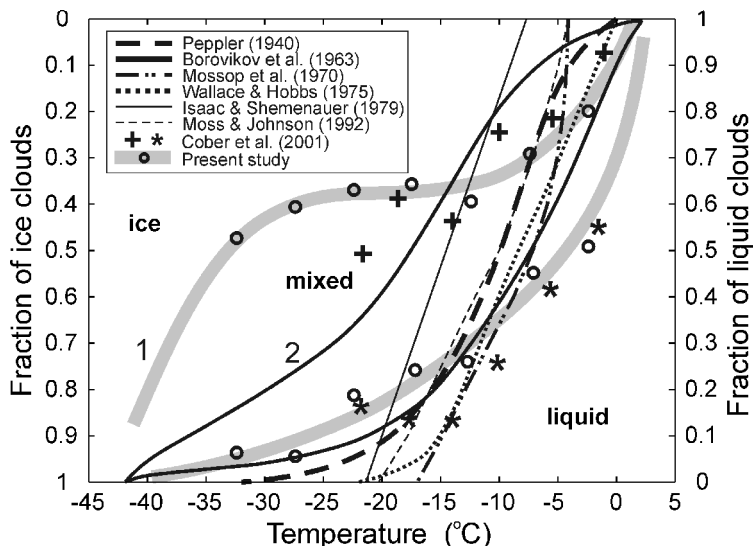


Figure 14. Comparison of fraction of ice, mixed- and liquid-clouds from the present and previous studies. Note that the left-hand and right-hand y-axes are in opposing senses. Lines labelled 1 and 2 should be referred to the left-hand axis and all other curves to the right-hand axis.

can produce alternate conclusions about the mixed-phase composition in different type of clouds.

#### (d) Mechanisms of ice nucleation in clouds

The concept of increasing activity of ice-forming nuclei with decreasing temperature has been demonstrated in numerous laboratory experiments (e.g. Roberts and Hallett 1968). The concept has been substantiated by observations of the increase of ice concentrations following the updraught in an ascending glider (Dye *et al.* 1986), and in aircraft penetrations at different levels in convective clouds. Data presented in Fig. 10 indicate that the average concentration of particles in ice clouds is a weak function of the ambient temperature. Moreover, there is a slight trend towards a decrease of ice-particle concentration as temperature decreases. This result seems contrary to the parametrizations of ice-forming nuclei (IFN) proposed by Fletcher (1962) and Meyers *et al.* (1992). Fletcher (1962) predicted an increase of ice-particle concentration of about nine orders of magnitude when the temperature dropped from  $-5^{\circ}\text{C}$  to  $-35^{\circ}\text{C}$ . The study of Meyers *et al.* (1992) proposed an increase of ice concentration approximately 100 times for the same temperature interval, reporting a concentration of ice particles of  $10^2\text{ l}^{-1}$  at  $-35^{\circ}\text{C}$ , which is less than one-tenth of the values we find at such temperatures. It is not believed that such a difference can be explained by the errors of measurements of particle concentration in the present work. Gultepe *et al.* (2001) showed a similar discrepancy between observations and parametrization.

The data presented here are collected in all different scenarios, since flight tracks are quite unrelated to cloud updraught/downdraught structure, and therefore must represent ice produced under situations other than simple nucleation. Rime splintering (Hallett and Mossop 1974) occurs over a narrow range of temperature ( $-3^{\circ}\text{C}$  to  $-8^{\circ}\text{C}$ ). However, Figs. 9 and 10 do not show any significant increase in concentration of ice particles in glaciated clouds warmer than  $-10^{\circ}\text{C}$ . Therefore it can be concluded that, *on average*, ice multiplication did not affect the concentration of ice particles in this dataset.

The global concept of ice concentration *averaged over a large area* irrespective of up- or down-draughts must result from processes, which are independent of temperature (such as evaporation break-up, Dong *et al.* 1994), together with a dispersal process which transports ice from areas of high concentrations to all levels of the atmosphere.

One could argue that the high concentration of ice at lower levels in the cloud may result from ice particles falling from layers above which are cooler and have a higher concentration of nucleated ice particles. However, this does not explain the high concentration of small ice-particles in shallow frontal cloud systems with cloud-top temperatures between  $-20^{\circ}\text{C}$  and  $-15^{\circ}\text{C}$ . It is also not clear how small ice-particles formed at  $-35^{\circ}\text{C}$  and having a low terminal fall velocity can consistently fall a few kilometres without a large change in their size.

One can hypothesize about the existence of a ‘universal’ mechanism of ice nucleation in stratiform clouds, which dominates over the direct formation of ice on ice nuclei (deposition nucleation) and ice multiplication. One of the possible candidates for this role is the formation of ice particles through the freezing of liquid droplets. Studies of nucleation in natural clouds have found that the freezing of liquid droplets appears to be the dominant mechanism in many clouds (Cooper and Vali 1981; Hobbs and Rangno 1985). According to this hypothesis, the formation of ice occurs in two stages. In the first, the vapour pressure exceeds the saturation pressure over water and liquid droplets get activated. In the second stage, droplet freezing occurs through activation of contact or immersion ice-nuclei. Recently, Cotton and Field (2002) numerically simulated ice nucleation in wave clouds as a result of homogeneous freezing (Jefferey and Austin, 1997), deposition (Meyers *et al.* 1992), contact nucleation (Young 1974) and immersion freezing (Bigg 1953). They found that none of the existing mechanisms of ice nucleation could reproduce the observed changes of the microstructure of wave clouds during their glaciation. From their observations, Cotton and Field (2002) found that glaciation occurs rapidly during droplet evaporation events.

Ice nucleation during evaporation may provide an attractive basis for a ‘universal’ mechanism of ice enhancement. This mechanism appears to be fairly general, since evaporation of droplets usually occurs in great numbers in downdraughts inside clouds and at cloud interfaces. Queen and Hallett (1990) and Rosinski and Morgan (1991) suggested that evaporating cloud droplets might provide an additional source of ice nuclei. The concept of ice nuclei, associated with solute nucleation following droplet evaporation, is particularly associated with the formation of eutectic\* as  $\text{NaCl}\cdot 2\text{H}_2\text{O}$ .

#### (e) *Spatial structure of mixed phase in clouds*

In this study, it has been assumed that liquid and ice particles are uniformly distributed in space and mix with each other in mixed-phase clouds. Such an assumption is rather idealistic, since inhomogeneities in cloud microstructure may, in some cases, exist all the way down to centimetre and sub-millimetre scales (Brenquier 1993; Baker *et al.* 2000). The resolution of modern aircraft instruments does not allow investigation of mixed-phase inhomogeneity on a scale smaller than about 100 metres (1 s). It is quite possible that phase inhomogeneity may exist down to metre or centimetre scales, i.e. fine scale clusters of liquid (ice) embedded in a glaciated (liquid) cloud.

In natural clouds, the ice and liquid may be well separated in space and located in clusters of liquid and ice only. From experimental evidence, Figs. 1, 3 and 13 show

\* (Chemistry) The isothermal transformation of a liquid solution simultaneously into different solid phases. In a system with just two constituents, such as NaCl and water, crystallization of both constituents occurs simultaneously, and at a unique temperature.

that such clusters exist at the scale of the order of kilometres. Hallett (1999) observed well-separated regions of ice and liquid in sea-breeze-front clouds. The ice and water regions extended some few kilometres up- and down-stream but the actual mixed-phase interface was of some few hundreds of metres wide. The interface is a region where ice is eroding into the water cloud; thus it is not a fixed but a dynamic interface. This concept may be extended to a smaller scale, such as might occur in a region of sheared stratocumulus, with a similar asymmetry. Another example might be a feeder-seeder situation with an overlying cirrus cloud producing crystals, which become somewhat randomly distributed as they fall, falling into a warm layer with originally no ice at all. Hence, the concept of ice scale-times differs according to the physical model. An extreme case is for ice to be produced uniformly and simultaneously throughout a supercooled cloud

## 7. CONCLUSIONS

The following results were obtained from this study:

(a) The frequency of occurrence of the phase-composition coefficient,  $\mu_3 = \text{IWC}/\text{TWC}$ , was obtained for seven 5 degC intervals for the temperature range of 0 °C to -35 °C. The frequency of occurrence of  $\mu_3$  was found to have explicit minima in the range  $0.1 < \mu_3 < 0.9$  and two maxima for  $\mu_3 < 0.1$  (liquid clouds) and  $\mu_3 > 0.9$  (ice clouds) in all temperature intervals.

(b) The observed frequency of occurrence of  $\mu_3$  suggests the typical glaciation time of clouds was much less than the residence time of cloud particles, i.e.  $\tau_{gl} \ll \tau_{resid}$ .

(c) On average, the IWC in glaciated clouds decreased from about  $0.1 \text{ g m}^{-3}$  at -5 °C to  $0.02 \text{ g m}^{-3}$  at -35 °C (Fig. 6(a)), and LWC in liquid clouds decreased from  $0.16 \text{ g m}^{-3}$  at -5 °C to  $0.08 \text{ g m}^{-3}$  at -35 °C (Fig. 6(b)). The IWC averaged over all clouds was found to be almost constant with temperature (Fig. 7).

(d) The average concentration of cloud particles measured by two FSSPs in glaciated clouds was found to be approximately constant at temperatures below -10 °C, varying in the range from  $2 \text{ cm}^{-3}$  to  $5 \text{ cm}^{-3}$ . The observation of a constant concentration of ice particles over all cloud temperatures may be interpreted as an indication that there exists a universal mechanism of ice formation in tropospheric clouds. No simple explanation of this observation was found, and further study is warranted.

(e) The average concentration of droplets measured by two FSSPs in liquid clouds was found to decrease with decreasing temperature, from approximately  $200 \text{ cm}^{-3}$  at -10 °C to  $30 \text{ cm}^{-3}$  at -35 °C.

(f) The average mean volume diameter  $\overline{D_3}$  in glaciated clouds varied between 20 and 35  $\mu\text{m}$  having a maximum around -15 °C, and then decreased as temperature decreased.

(g) No spatial correlation between LWC and IWC was found in stratiform clouds. On average, the correlation coefficient between LWC and IWC varied between  $\pm 0.3$ .

## ACKNOWLEDGEMENTS

The authors appreciate useful comments of anonymous reviewers. The Panel on Energy Research and Development provided financial support for BASE and FIRE.ACE. Additional support for the collection of the FIRE.ACE data was given by NASA. The National Search and Rescue Secretariat of Canada, Boeing Commercial Airplane Group, Transport Canada, and the Canadian Department of National Defense provided funding

for the CFDE and AIRS projects. The aircraft data were obtained using the scientific and technical efforts of many NRC and MSC staff. The assistance of M. Wasey, S. Bacic, and S. Krickler of MSC and D. L. Marcotte of NRC in conducting the field projects is gratefully acknowledged. Alexei Korolev performed this work under contract KM175-012030/001/TOR to the Meteorological Service of Canada. The Panel of Energy Research and Development, and the National Search and Rescue Secretariat provided funding for this work. John Hallett was supported by grant ATM-9900560, Physical Meteorology Program, National Science Foundation, Arlington VA and NASA grant NAG-1-2046.

## REFERENCES

- Arnott, W. P., Mitchell, D. L., Shmitt, C., Kingsmill, D., Ivanova, D. and Poellot, M. 2000 'Analysis of the FSSP performance for measurement of small crystal spectra in cirrus clouds'. Pp. 191–193 in *Proceedings of 13th International Conference on clouds and precipitation*, Reno, Nevada, USA, 14–18 August, 2000
- Baker, B. A., Lawson, P. R. and Schmitt, C. G. 2000 'Clumpy cirrus'. Pp. 637–640 in *Proceedings of 13th International Conference on clouds and precipitation*, Reno, Nevada, USA, 14–18 August, 2000
- Bigg, E. K. 1953 The formation of atmospheric ice crystals by the freezing of droplets. *Q. J. R. Meteorol. Soc.*, **79**, 510–519
- Biter, C. J., Dye, J. E., Huffman, D. and King, W. D. 1987 The drop-size response of the CSIRO liquid water probe. *J. Atmos. Oceanic Technol.*, **4**, 359–367
- Borovikov, A. M., Gaivoronskii, I. I., Zak, E. G., Kostarev, V. V., Mazin, I. P., Minervin, V. E., Khrgian, A. Kh. and Shmeter, S. M. 1963 P. 393 in *Cloud physics*. Israel program of scientific translations, Jerusalem, Israel
- Brenguier, J. L. 1993 Observations of cloud microstructure at the centimetre scale. *J. Appl. Meteorol.*, **32**, 783–793
- Brown, P. A. 1993 Measurements of the ice-water content in cirrus using an evaporative technique. *J. Atmos. Oceanic Technol.*, **2**, 340–352
- Cober, S. G., Isaac, G. A. and Korolev, A. V. 2000 'Assessing the relative contribution of liquid and ice phases in winter clouds'. Pp. 689–693 in *Proceedings of 13th International Conference on clouds and precipitation*, Reno, Nevada, USA, 14–18 August, 2000
- 2001a Assessing the Rosemount icing detector with in situ measurements. *J. Atmos. Oceanic Technol.*, **18**, 515–528
- 2001b Assessing cloud phase conditions. *J. Appl. Meteorol.*, **40**, 1967–1983
- Cooper, W. A. and Vali, G. 1981 The origin of ice in mountain cap clouds. *J. Atmos. Sci.*, **38**, 1244–1259
- Cotton, R. J. and Field, P. R. 2002 Ice nucleation characteristics of an isolated wave cloud. *Q. J. R. Meteorol. Soc.*, **128**, 2417–2437
- Dong, Y. Y., Oraltay, R. G. and Hallett, J. 1994 Ice-particle generation during evaporation. *Atmos. Res.*, **32**, 45–53
- Dye, J. E., Jones, J. J., Winn, W. P., Cerni, T. A., Gardiner, B., Lamb, D., Pitter, R. L., Hallett, J. and Saunders, C. 1986 Early electrification and precipitation development in a small, isolated Montana cumulonimbus. *J. Geophys. Res.*, **91**, 1221–1247
- Field, P. R., Wood, R., Brown, P. R. A., Kaye, P., Hirst, E., Greenaway, R. and Smith, J. A. 2002 Ice-particle interarrival time measured with fast FSSP. *J. Atmos. Oceanic Technol.* In press
- Fletcher, N. H. 1962 *Physics of Rain Clouds*. Cambridge University Press, Cambridge, UK
- Gayet, J. F., Febvre, G. and Larsen, H. 1996 The reliability of the PMS FSSP in the presence of small ice crystals. *J. Atmos. Oceanic Technol.*, **13**, 1300–1310
- Gultepe, I., Isaac, G. A. and Cober, S. G. 2001 Ice crystal number concentration versus temperature. *Int. J. Climatol.*, **21**, 1281–1302

- Hallett, J. 1976 'Measurement of size, concentration, and structure of atmospheric ice particles by the airborne continuous particle replicator'. AFGL-TR-76-0149 Airforce Geophysics Laboratory, Hanscom AFB, MA 01731, USA
- Hallett, J. 1999 'Charge generation with and without secondary ice production'. Pp. 355–358 in *Proceedings of 11th International Conference on atmospheric electricity*, NASA/CP-1999-209261, June, Huntsville, Alabama, USA
- Hallett, J. and Isaac, G. A. 2002 'Aircraft icing in glaciated and mixed phase clouds', in *AIAA 40th aerospace science meeting and exhibit*, Reno, Nevada, USA, 14–17 January 2002, American Institute of Aeronautics and Astronautics-2002-0677. Available from <http://www.aiaa.org/publications/ind ex.hfm?pub=0>
- Hallett, J. and Mossop, S. C. 1974 Production of secondary particles during the riming process. *Nature*, **249**, 26–28
- Heymsfield, A. 1972 Ice crystal terminal velocities. *J. Atmos. Sci.*, **29**, 1348–1357
- Heymsfield, A. J. and Platt, C. M. R. 1984 A parametrization of the particle size spectrum of ice clouds in terms of the ambient temperature and the ice-water content. *J. Atmos. Sci.*, **41**, 846–855
- Hobbs, P. V. and Rangno, A. L. 1985 Ice-particle concentrations in clouds. *J. Atmos. Sci.*, **42**, 2523–2549
- Isaac, G. A. and Schemenauer, R. S. 1979 Large particles in supercooled regions of northern Canadian cumulus clouds. *J. Appl. Meteorol.*, **18**, 1056–1065
- Ivanova, D., Mitchell, D. L., Amott, W. P. and Poellot, M. 2001 A GCM parametrization for bimodal size spectra and ice mass removal rates in mid-latitude cirrus clouds. *Atmos. Res.*, **59–60**, 89–113
- Jeffrey, C. A. and Austin, P. H. 1997 Homogeneous nucleation of supercooled water: Results from a new equation state. *J. Geophys. Res.*, **102**(D21), 25269–25279
- Jiang, H., Cotton, W. R., Pinto, J. O., Curry, J. A. and Weissbluth, M. J. 2000 Cloud resolving simulations of mixed-phase Arctic stratus observed during BASE: sensitivity to concentration of ice crystals and large-scale heat and moisture advection. *J. Atmos. Sci.*, **57**, 2105–2117
- King, W. D., Parkin, D. A. and Handsworth, R. J. 1978 A hot-wire water device having fully calculable response characteristics. *J. Appl. Meteorol.*, **17**, 1809–1813
- Knollenberg, R. G. 1981 'Techniques for probing cloud microstructure'. In *Clouds, their formation, optical properties, and effects*, Eds. P. V. Hobbs and A. Deepak, Academic Press, New York, USA
- Korolev, A. V. 1998 'About a definition of liquid, mixed and ice clouds'. Pp. 325–326 in *Proceedings of FAA Workshop on mixed-phase and glaciated icing conditions*, 2 & 3 Dec. 1998, Federal Aviation Authority, Atlantic City, NJ, USA
- Korolev, A. V. and Isaac, G. A. 1998 'Phase composition of stratiform clouds'. Pp. 129–146 in *Proceedings of FAA Workshop on mixed-phase and glaciated icing conditions*, 2 & 3 Dec. 1998, Federal Aviation Authority, Atlantic City, NJ, USA
- 2000 'Phase composition of stratiform clouds'. Pp. 725–727 in *Proceedings of 13th Int. Conf. on clouds and precipitation*, Reno, Nevada, USA, 14–18 August, 2000
- 2002a Phase transformation of mixed-phase clouds. *Q. J. R. Meteorol. Soc.*, **129**, 19–38
- 2002b Roundness and aspect ratio of particles in ice clouds. *J. Atmos. Sci.* In press
- Korolev, A. V. and Strapp, J. W. 2002 'Accuracy of measurements of cloud ice content by the Nevzorov probe', in *AIAA 40th aerospace science meeting and exhibit*, Reno, Nevada, USA, 14–17 January 2002, American Institute of Aeronautics and Astronautics-2002-0679. Available from <http://www.aiaa.org/publications/ind ex.hfm?pub=0>
- Korolev, A. and Sussman, B. 2000 A technique for habit classification of cloud particles. *J. Atmos. Oceanic Technol.*, **17**, 1048–1057
- Korolev, A. V., Strapp, J. W., Isaac, G. A. and Nevzorov, A. N. 1998 The Nevzorov airborne hot-wire LWC-TWC probe: principle of operation and performance characteristics. *J. Atmos. Oceanic Technol.*, **15**, 1495–1510
- Korolev, A., Isaac, G. A. and Hallett, J. 2000 Ice-particle habits in stratiform clouds. *Q. J. R. Meteorol. Soc.*, **126**, 2873–2902
- Korolev, A., Isaac, G. A., Mazin, I. P. and Barker, H. 2001 Microphysical properties of continental clouds from *in situ* measurements. *Q. J. R. Meteorol. Soc.*, **127**, 2117–2151

- Lawson, P. R., Baker, B., Schmitt, C. G. and Jensen, T. 2001 An overview of microphysical properties of Arctic clouds observed in May and June 1998 during FIRE ACE. *J. Geophys. Res.*, **106**, 14989–15014
- Lohmeier, S. P., Sekelsky, S. M., Firda, J. M., Sadowy, G. A. and McIntosh, R. E. 1997 Classification of particles in stratiform clouds using the 33 and 95 GHz polarimetric cloud profiling radar system (CPRS). *IEEE Transactions on Geoscience and Remote Sensing*, **35**, 256–270
- Mason, B. J. 1994 The shapes of snow crystals—Fitness for purpose? *Q. J. R. Meteorol. Soc.*, **120**, 849–860
- Mazin, I. P., Nevzorov, A. N., Shugaev, V. P. and Korolev, A. V. 1992 ‘Phase structure of stratiform clouds’. Pp. 332–336 in *Proceedings of 11th Int. Conf. on clouds and precipitation*, Montreal, Canada, 17–21 August, 1992
- Mazin, I. P., Korolev, A. V., Heymsfield, A., Isaac, G. A. and Cober, S. G. 2001 Thermodynamics of icing cylinder for measurements of liquid water content in supercooled clouds. *J. Atmos. Oceanic Technol.*, **18**, 543–558
- Meyers, M. P., DeMott, P. J. and Cotton, W. R. 1992 New primary ice-nucleation parametrizations in an explicit cloud model. *J. Appl. Meteorol.*, **31**, 708–721
- Moss, S. J. and Johnson, D. W. 1994 Aircraft measurements to validate and improve numerical model parametrization of ice to water ratios in clouds. *Atmos. Res.*, **34**, 1–25
- Mossop, S. C., Ono, A. and Wishart, E. R. 1970 Ice particles in maritime clouds near Tasmania. *Q. J. R. Meteorol. Soc.*, **96**, 487–508
- Nevzorov, A. N. 1980 ‘Aircraft cloud water content meter’. Pp. 701–703 in vol. II of *Comm. à la 8eme conférence internationale sur la physique des nuages*, Clermont-Ferrand, France
- 1983 ‘Aircraft cloud water content meter’. (In Russian). Pp. 19–26 in *Transactions of Central Aerological Observatory (Trudi TsAO)*, **147**
- 2000 ‘Cloud phase composition and phase evolution as deduced from experimental evidence and physico-chemical concepts’. Pp. 728–731 in *Proceedings of 13th Int. Conf. on clouds and precipitation*, Reno, Nevada, USA, 14–18 August, 2000
- Oshchepkov, S. and Isaka, H. 1998 Inverse scattering problem for mixed-phase and ice clouds. Part I: Numerical simulation of particle sizing from phase-function measurements. *Appl. Opt.*, **36**, 8765–8774
- Peppler, W. 1940 Unterkühlte Wasserwolken und Eiswolken. *Forsch. und Erfahrung*, Reichsamt für Wetterdienst. B., No 1
- Pueschel, R. F., Hallett, J., Strawa, A. W., Howard, S. D., Ferry, G. V., Foster, T. and Amott, W. P. 1997 Aerosol and cloud particles in tropical cirrus anvil: importance to radiation balance. *J. Aerosol Sci.*, **28**, 1123–1136
- Queen, B. and Hallett, J. 1990 ‘Crystallization of highly supersaturated solutions’. Pp. 97–100 in *Proceedings of AMS Conference on cloud physics*, San Francisco, CA, USA
- Roberts, P. and Hallett, J. 1968 A laboratory study of the ice nucleating properties of some mineral particulates. *Q. J. R. Meteorol. Soc.*, **94**, 25–34
- Rosinski, J. and Morgan, G. 1991 Cloud condensation nuclei as a source of ice forming nuclei in clouds. *J. Aerosol Sci.*, **122**, 123–133
- Ryan, B. F., Wishart, E. R. and Shaw, D. E. 1976 The growth rates and densities of ice crystals between  $-3^{\circ}\text{C}$  and  $-21^{\circ}\text{C}$ . *J. Atmos. Sci.*, **33**, 53–70
- Schols, J. L., Weinman, J. A., Alexander, G. D., Stewart, R. E., Angus, L. J. and Lee, A. C. L. 1999 Microwave properties of frozen precipitation around a North Atlantic cyclone. *J. Appl. Meteorol.*, **38**, 29–43
- Strapp, J. W., Chow, P., Maltby, M., Beezer, A. D., Korolev, A. V., Stronberg, I. and Hallett, J. 1999 ‘Cloud microphysical measurements in thunderstorm outflow regions during Allied/BAE 1997 flight trials’ in *AIAA 37th Aerospace Sci. meeting and exhibit*, Reno, Nevada, USA, 11–14 January 1999, American Institute of Aeronautics and Astronautics-99-0498. Available from <http://www.aiaa.org/publications/index.htm?pub=0>
- Strapp, J. W., Oldenburg, J., Ide, R., Lilie, L., Bacic, S., Vukovic, Z., Oleskiw, M., Miller, D., Emery, E. and Leone, G. 2002 Wind tunnel measurements of the response of hot-wire liquid water content instruments to large droplets. *J. Atmos. Oceanic Technol.* In press

- Sun, Z. and Shine, K. P. 1995 Parametrization of ice cloud radiative properties and its application to the potential climatic importance of mixed-phase clouds. *J. Climate*, **8**, 1874–1888
- Tremblay, A., Glazer, A., Benoit, W. and Yu, R. 1996 A mixed-phase cloud scheme based on a single prognostic equation. *Tellus.*, **48**, 483–500
- Twohy, C. H., Schanot, A. J. and Cooper, W. A. 1997 Measurement of condensed water content and ice clouds using an airborne counterflow virtual impactor. *J. Atmos. Oceanic Techn.*, **14**, 197–202
- Vali, G. 1971 Quantitative evaluation of experimental results on the heterogeneous freezing nucleation of supercooled liquids. *J. Atmos. Sci.*, **28**, 402–408
- Wallace, J. M. and Hobbs, P. V. 1975 *Atmospheric Science: An introductory survey*. Academic Press, New York, USA
- Weickmann, H. 1945 Formen und Bildung atmosphärischer Eiskristalle. *Beitr. Phys.Frei Atmos.*, **28**, 12–552
- Wilson, D. 2000 The impact of a physically based microphysical scheme on the climate simulation of the Meteorological Office Unified Model. *Q. J. R. Meteorol. Soc.*, **126**, 1281–1300
- Williams, E., Zhang, R. and Rydock, J. 1991 Mixed-phase microphysics and cloud electrification. *J. Atmos. Sci.*, **48**, 2195–2203
- Young, K. C. 1974 The role of contact nucleation in ice phase initiation in clouds. *J. Aerosol Sci.*, **31**, 768–776
- Young, S. A., Platt, C. M. R., Austin, R. T. and Patterson, G. R. 2000 Optical properties and phase of some mid-latitude, mid-level clouds in ECLIPS. *J. Appl. Meteorol.*, **39**, 135–153
- Zak, E. G. 1937 A characterization of frontal clouds using aircraft soundings. *Soviet Meteorology and Hydrology*, **8**, 15–28